



Northern Lights on Food Masterclass

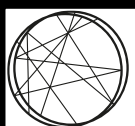
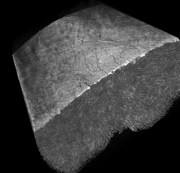
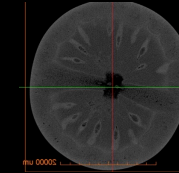
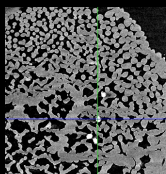
IMAGING MICROSTRUCTURES OF FOOD AND PACKAGING WITH X-RAYS AND NEUTRONS

Stephen Hall

*Lund Institute of advanced Neutron and X-ray Science (LINXS)
& Division of Solid Mechanics, Lund University, Sweden
& 4D Imaging Lab @Lund University*



4D IMAGING LAB



LUND INSTITUTE OF ADVANCED
NEUTRON AND X-RAY SCIENCE

LINXS



Why do x-ray and neutron imaging?...
what's happening inside?...



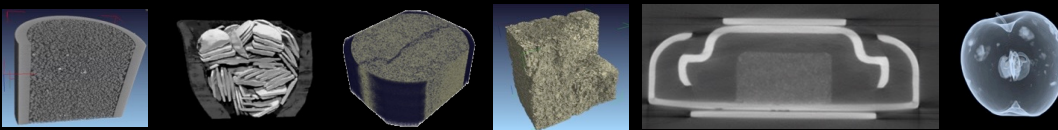
By normal visual inspection, we have no idea...

Why do x-ray and neutron imaging?...
what's happening inside?...



Objectives:

- Introduce neutron and x-ray imaging
- Describe some of the details of x-ray and neutron tomography
- Demonstrate the usage of x-ray and neutron imaging with applications to food and packaging



History

RADIOGRAPHY

- Discovery of X-rays by Wilhelm Röntgen
- First radiographies in 1895
- First Nobel prize in Physics in 1901



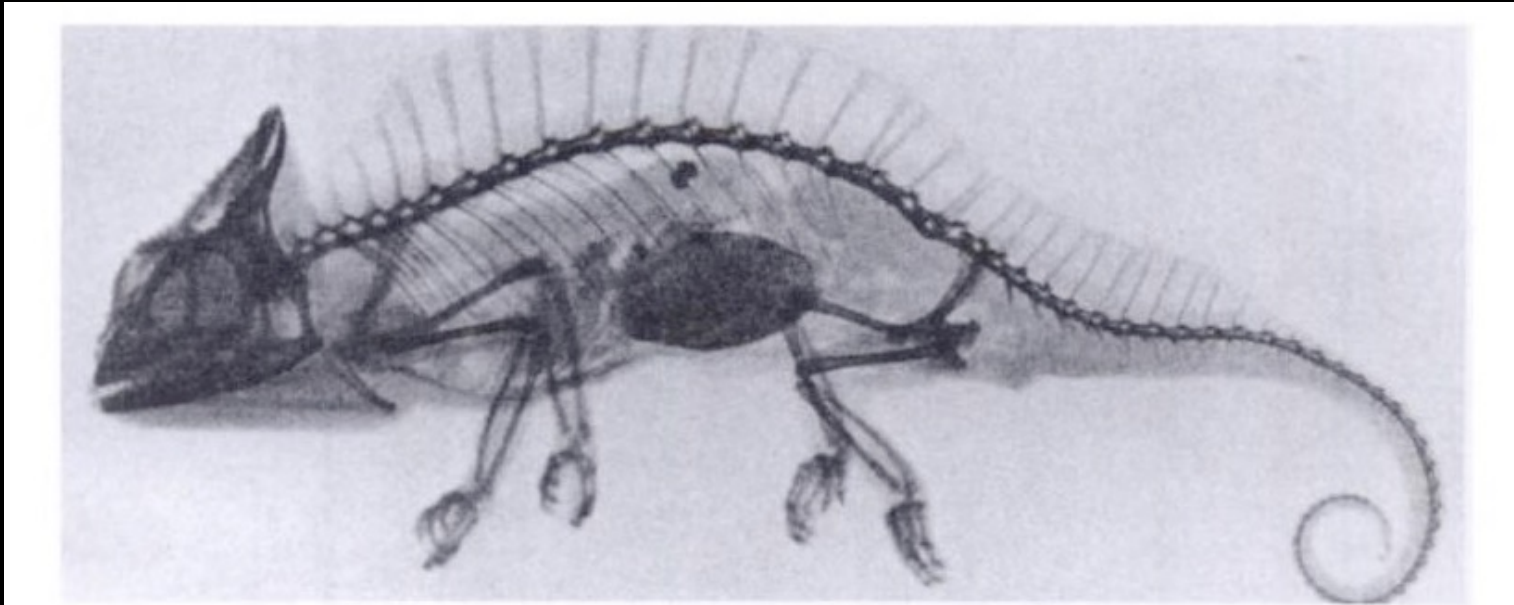
Hand mit Ringen (Hand with Rings): print of Wilhelm Röntgen's first "medical" X-ray, of his wife's hand, taken on 22 December 1895 and presented to Professor Ludwig Zehnder of the Physik Institut, University of Freiburg, on 1 January 1896

(<http://en.wikipedia.org/wiki/X-ray>)

History

RADIOGRAPHY

- Discovery of X-rays by Wilhelm Röntgen
- First radiographies in 1895
- First Nobel prize in Physics in 1901



February 1896 - African chameleon

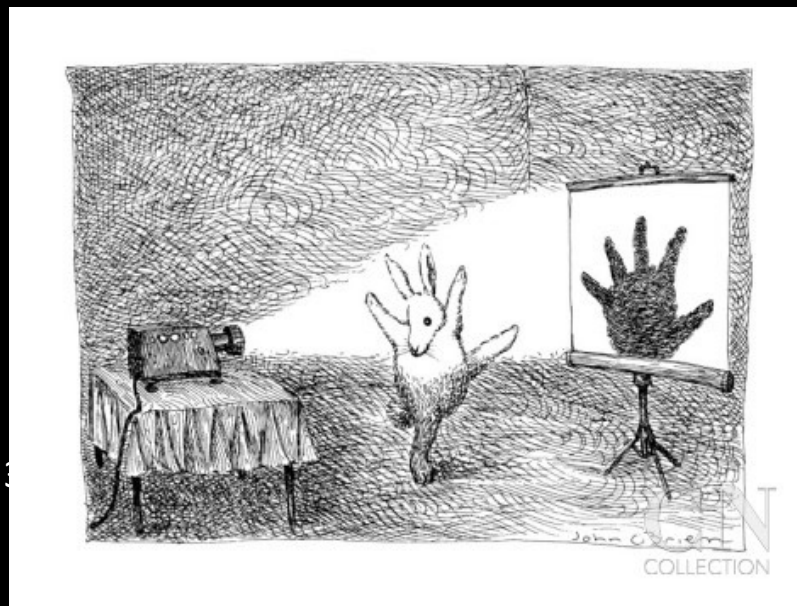
2D → 3D imaging

radiography vs. tomography



when the detail to be observed (here, a fracture) is in the plane of the radiography, this can be sufficient (for medical diagnosis in this case)

But this can be misleading...



When things must be seen in 3D,
radiography is not sufficient

History

TOMOGRAPHY

- Tomography = “extension” of radiography
- The original mathematical framework by Radon in 1917
- First X-ray CT scanner in 1972 by Hounsfield in collaboration with Cormack
- Nobel prize in Medicine in 1979



Godfrey N. Hounsfield with a medical “CT” scanner
(www.betterproductdesign.net)

X-ray tomography machines

X-RAY SOURCE + DETECTOR + SYSTEM FOR THE MULTI-ANGLE MEASUREMENT

3 main types of machines for X-ray tomography:
Medical ("CT"), lab/industrial and synchrotron



Medical scanner
e.g., LBIC



Lab/Industrial scanner
e.g., 4D Imaging Lab



Synchrotron
e.g., MAXIV

X-RAY TUBE

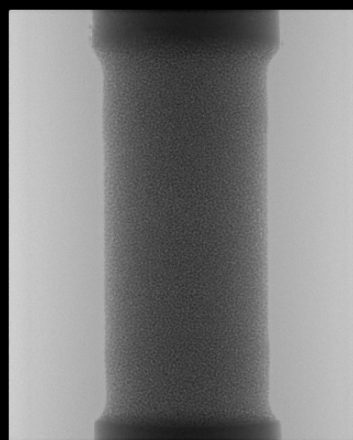
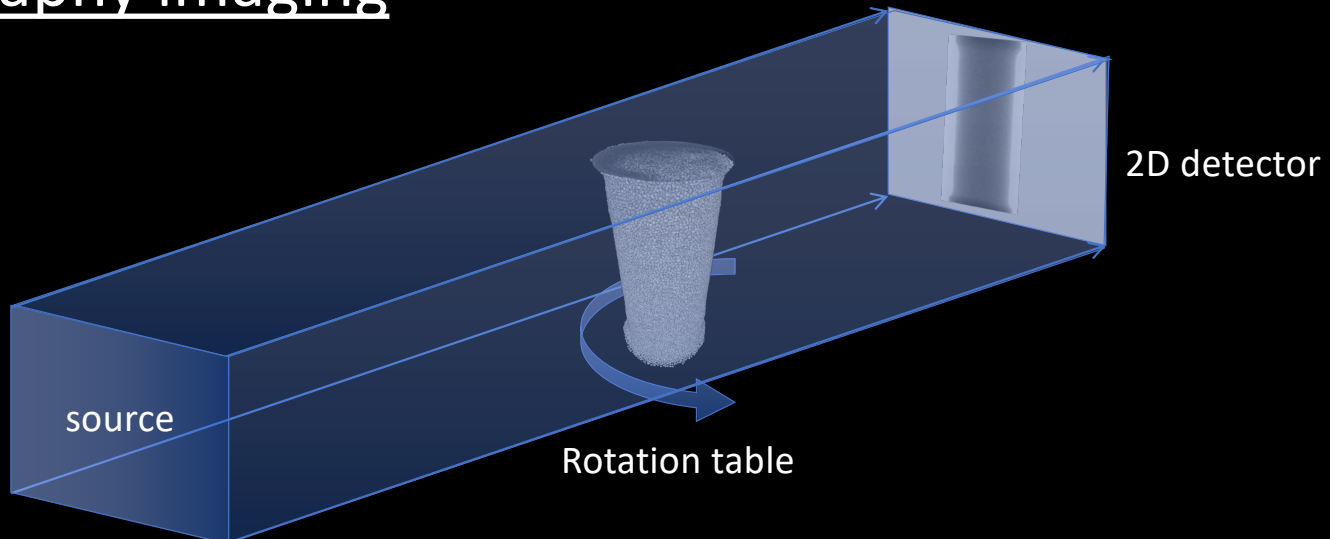
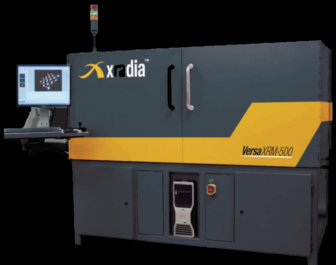
**ACCELERATED
ELECTRONS**

Comparison between X-ray tomography machines

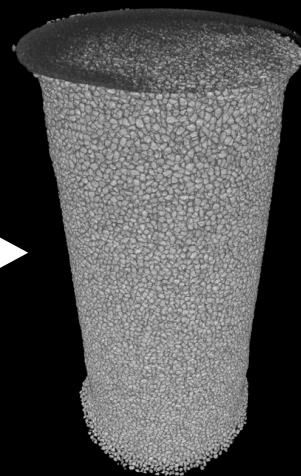
| Type of tomograph | Medical | Industrial/lab | Synchrotron |
|----------------------|-----------------------|-----------------------|--------------------------|
| X-ray source | X-ray tube | | Accelerator of electrons |
| Geometry beam | Fan or cone beam | | Parallel beam |
| Resolution | 100-500 μm | 0.5-100 μm | 0.1-10 μm |
| Object size | dm | mm-cm | μm -mm |
| Scanning time | sub.-sec to mins | 10's mins to hrs | seconds to mins |

- Best resolution with industrial/lab scanners and synchrotron.
- Best scanning time with medical scanners and synchrotron.
- Synchrotron - Best conditions for slice reconstruction (i.e. parallel and monochromatic beam) BUT generally small specimen size and difficult to obtain experiment time.
- Note that rapid advances are being made (30-50 nm in one lab tomograph (Xradia) but for VERY small samples) and MAXIV, NINA-ESRF...

Full field Tomography imaging



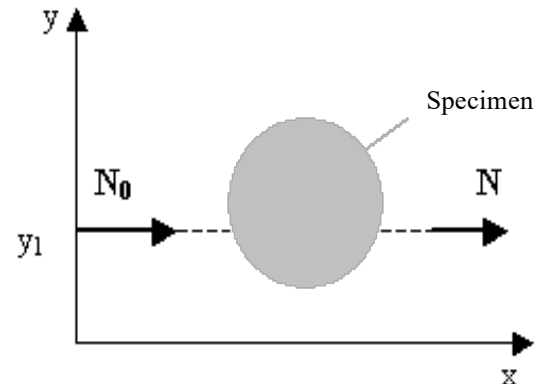
Reconstruction



Principle of transmission measurements (x-rays)

X-ray tomography uses the fact that X-rays are attenuated when they go through an object: one part is scattered, an another absorbed and the rest transmitted.

Beer-Lambert attenuation law



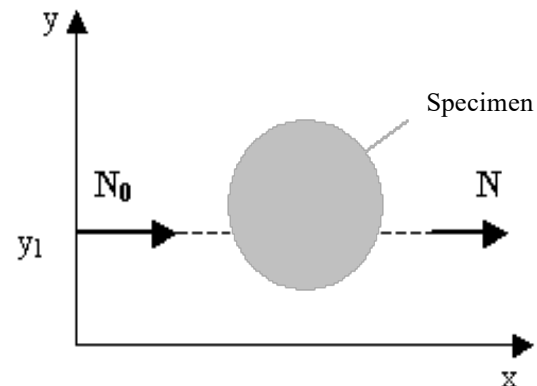
$$N = N_0 e^{-\left(\int_r^s \mu(x, y_1) dx \right)}$$

N_0 number of emitted photons
 N number of recorded photons
 μ linear attenuation coefficient

Principle of transmission measurements (x-rays)

X-ray tomography uses the fact that X-rays are attenuated when they go through an object: one part is scattered, an another absorbed and the rest transmitted.

Beer-Lambert attenuation law



$$N = N_0 e^{-\left(\int_r^y \mu(x, y_1) dx \right)}$$

N_0 number of emitted photons
 N number of recorded photons
 μ linear attenuation coefficient

$$\mu = \rho \left[a \underbrace{\frac{Z^m}{E^n A}}_{\text{Photoelectric absorption}} + b \underbrace{\frac{Z}{A}}_{\text{Compton scattering}} \right]$$

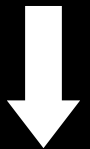
E : X-ray energy
 ρ : mass density
Z : atomic number
A : atomic weight
m, n, a and b : constants

Principle of transmission measurements (x-rays)

Linear attenuation coefficient

$$\mu = \rho \left[a \underbrace{\frac{Z^m}{E^n A}}_{\text{Photoelectric absorption}} + b \underbrace{\frac{Z}{A}}_{\text{Compton scattering}} \right]$$

E : X-ray energy
ρ : mass density
Z : atomic number
A : atomic weight
m, n, a and b : constants



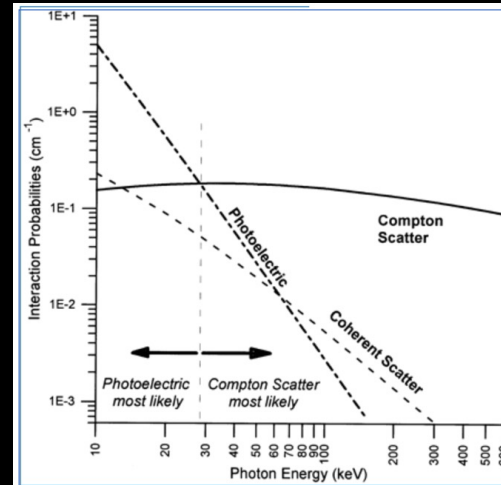
$$\mu = \rho \left[a \frac{Z^{3.8}}{E^{3.2}} + b \right]$$

As Z/A is roughly constant and m and n can be determined for most of the materials and energies used

Linear attenuation coefficient

$$\mu = \rho \left[a \frac{Z^{3.8}}{E^{3.2}} + b \right]$$

*Photoelectric Compton
absorption scattering*



$E < 30 \text{ keV} \rightarrow$ Photoelectric absorption is predominant so :

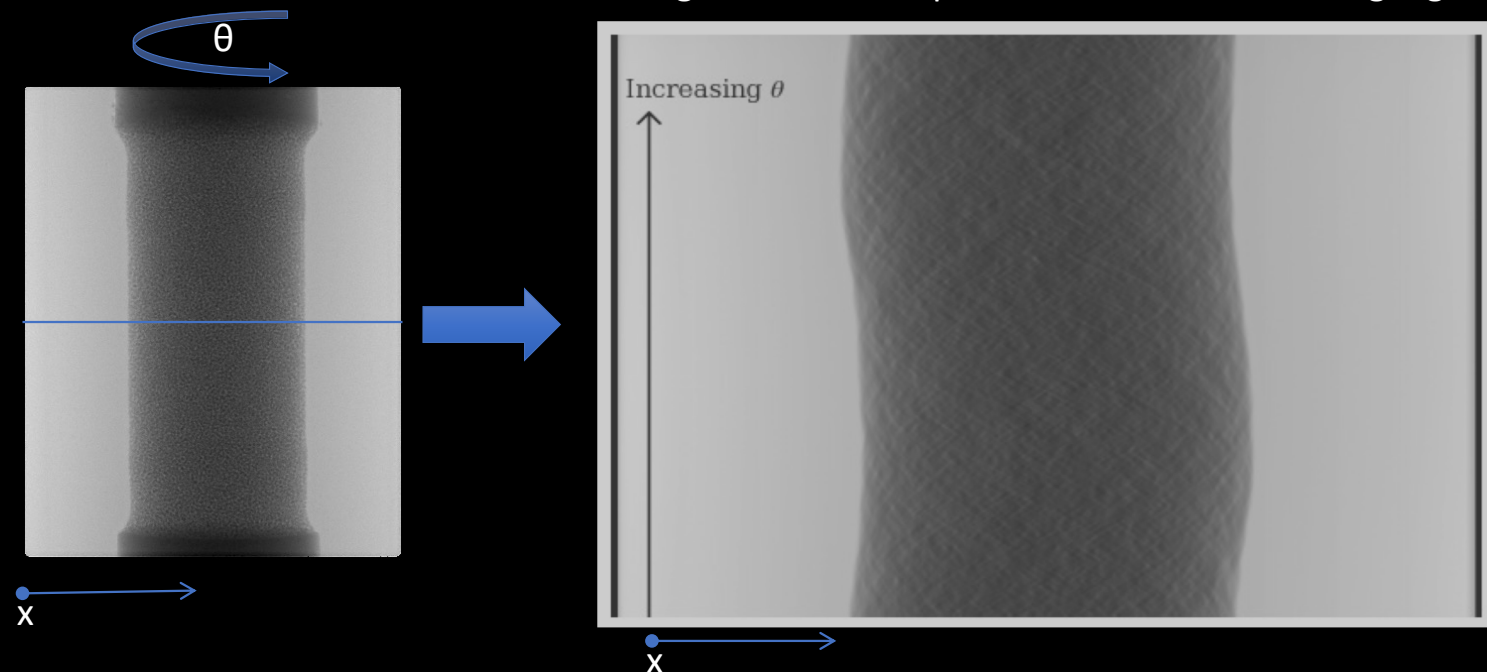
1. comparing density in two different zones in the object is only possible if the atomic number Z is constant
2. a change in density between two zones can be cancelled by a change of the atomic number in the opposite direction

$E > 30 \text{ keV} \rightarrow$ Compton scattering is predominant so μ is only related to mass density BUT contrast within the image is lower:

(variation with keV is material dependent)

Tomography methodology

We reconstruct the 3D image slice by slice

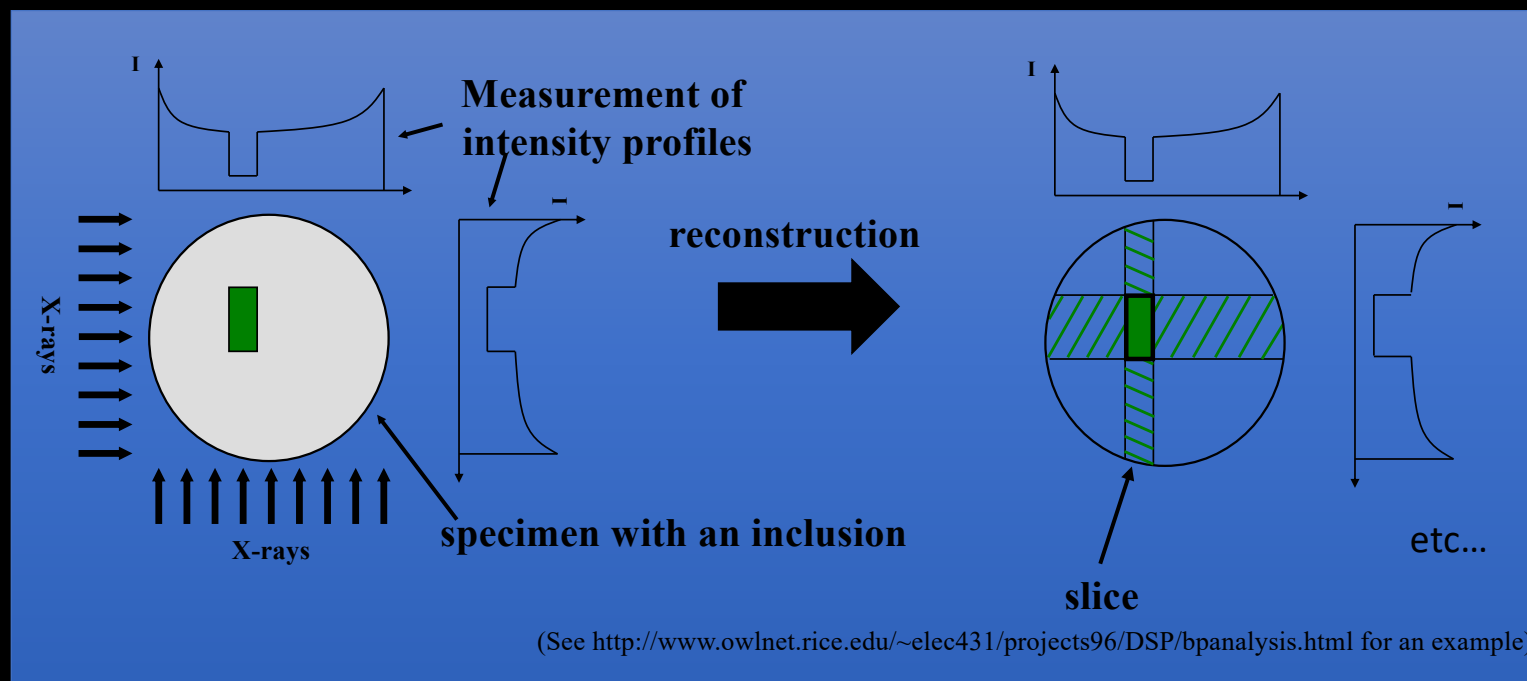


This is a sinogram - a Radon transform of the slice

Images: E. Andò
Lab 3SR, Grenoble

Principle of reconstruction

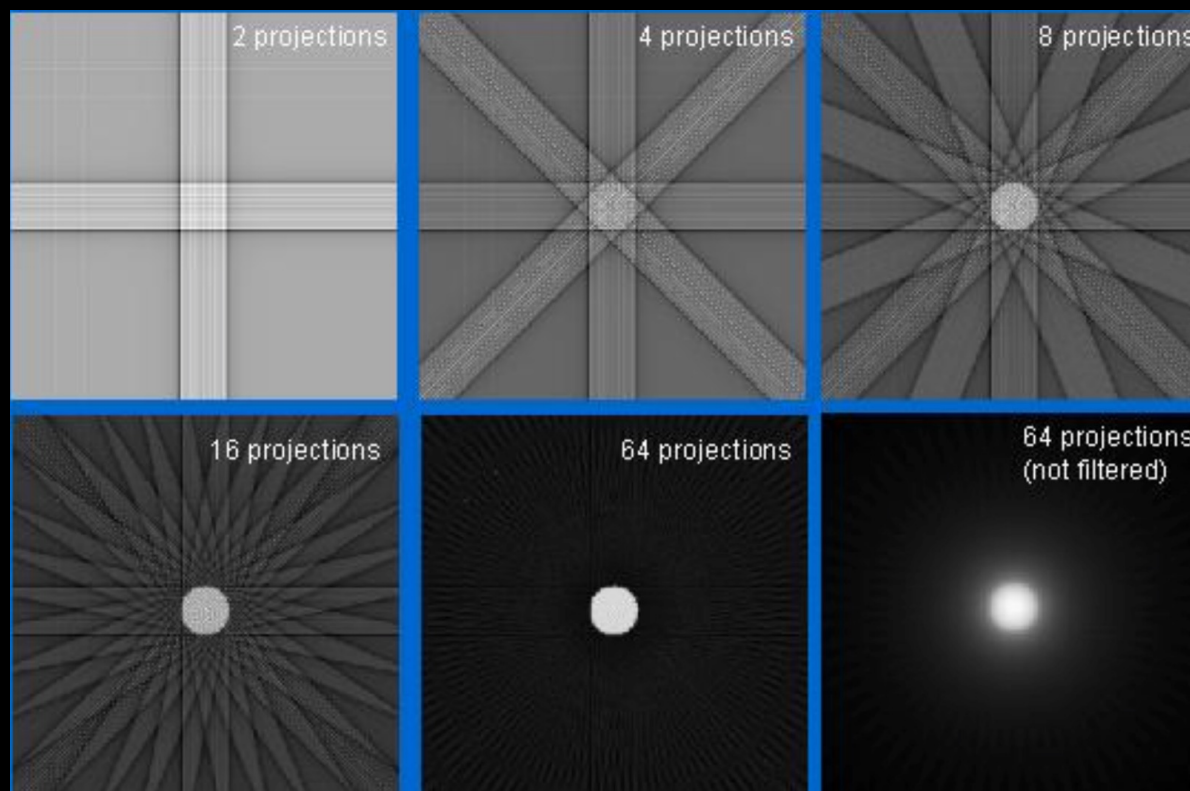
- Reconstruction of slices from different angle measurements with appropriate algorithm (analytic or algebraic methods), basic approach is back-projection:



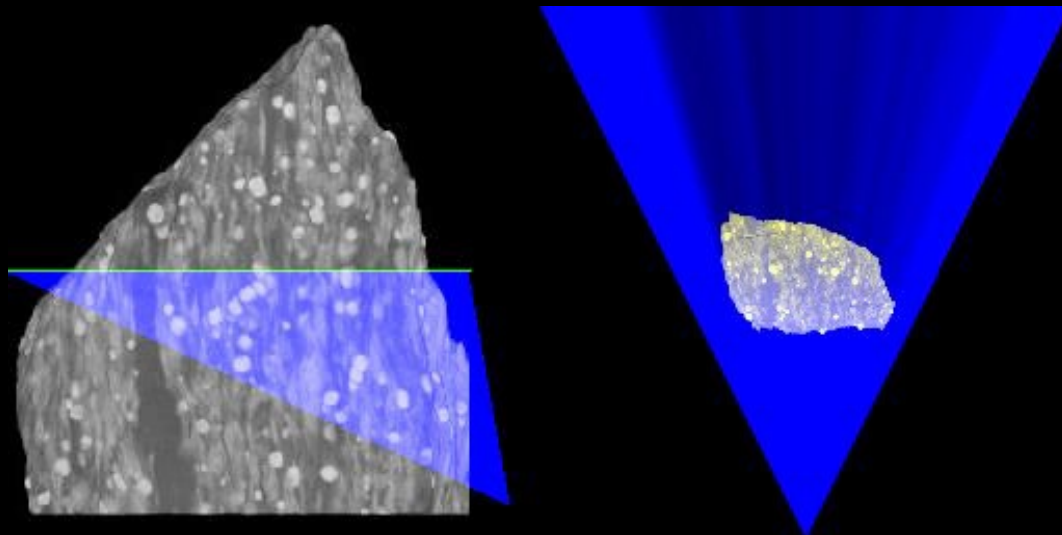
$$N = N_0 e^{-\left(\int_r \mu(x, y_1) dx \right)}$$

Principle of reconstruction

- Reconstruction of slices from different angle measurements with appropriate algorithm (analytic or algebraic methods), basic approach is back-projection:

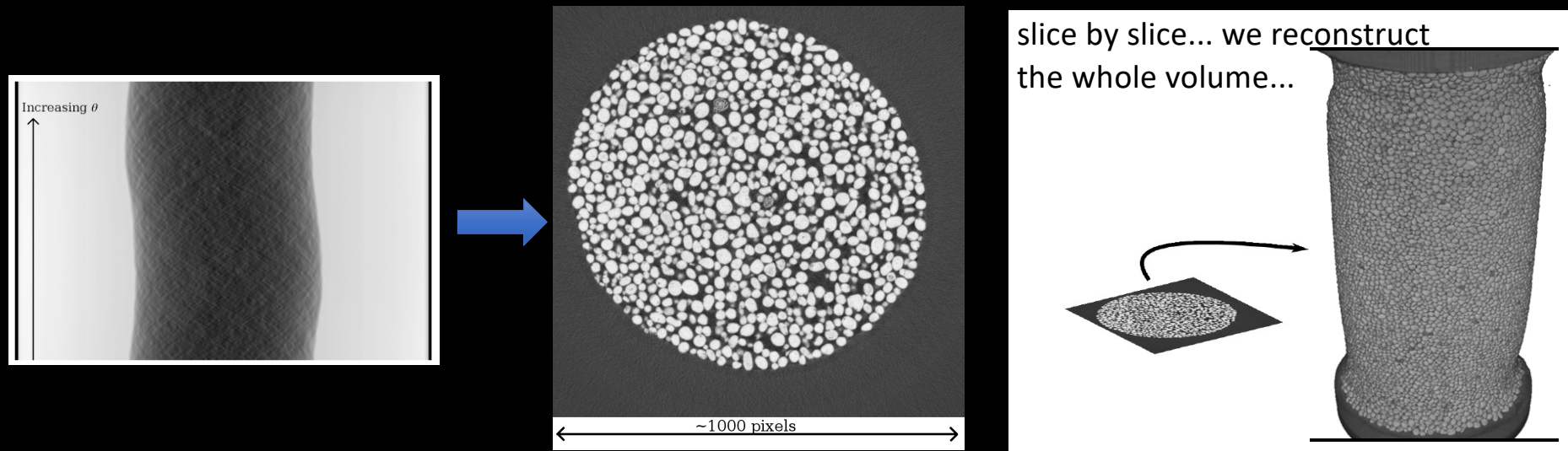


Principle of reconstruction



Principle of reconstruction

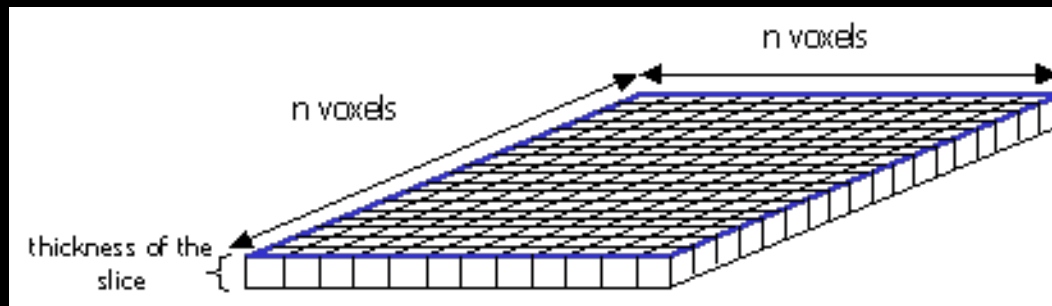
Knowing the centre of rotation we can solve the inverse problem (inverse radon transform), which results in a reconstruction of the slice that gave rise to the sinogram



Images: E. Andò
Lab 3SR, Grenoble

Voxel = pixel in 3D

Each slice represents a finite thickness of the object and is composed of voxels (extension in 3D of a pixel).

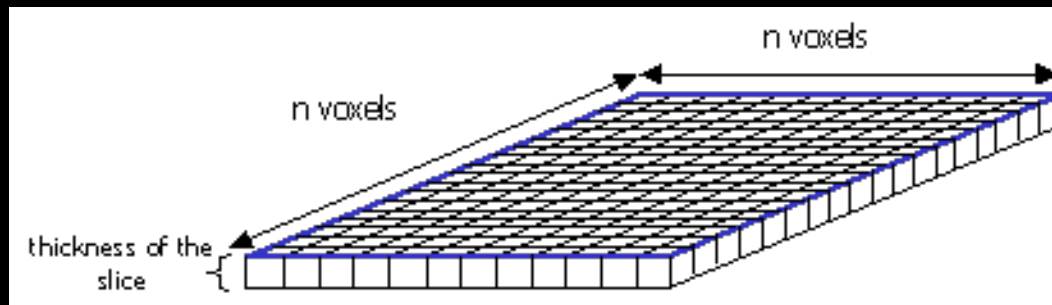


Schematic of a slice (composed of $n \times n$ voxels)

The final parameter visualised i.e., voxel values in the reconstructed slice, is linked to the mean of the linear attenuation coefficients of all the components physically presents in the voxel.

Voxel = pixel in 3D

Each slice represents a finite thickness of the object and is composed of voxels (extension in 3D of a pixel).



Schematic of a slice (composed of $n \times n$ voxels)

The final parameter visualised i.e. voxel values in the reconstructed slice, is linked to the mean of the linear attenuation coefficients of all the components physically presents in the voxel.

The size of the voxel is the **image “discretisation”**...

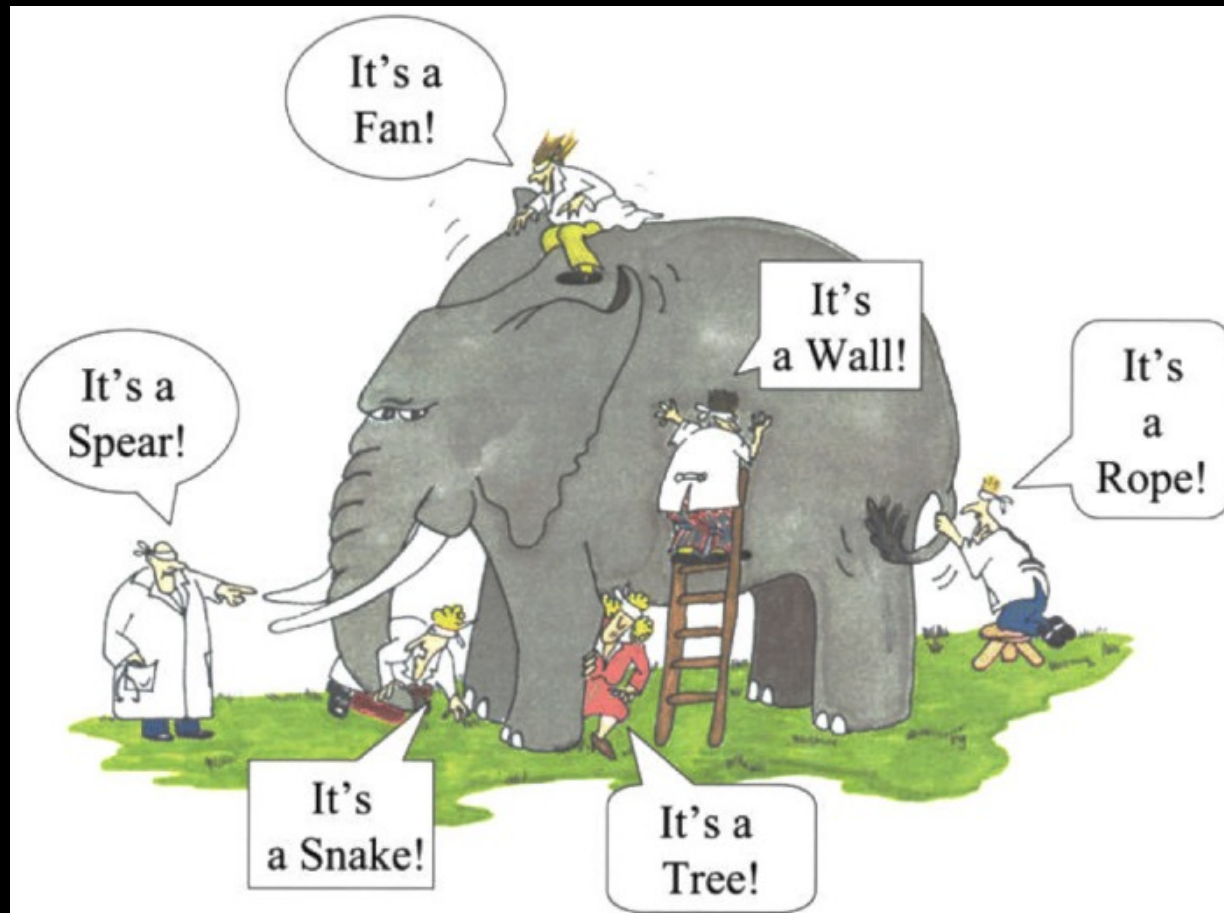
... this is not the **spatial resolution** as is commonly said...

... spatial resolution will be a function of the reconstruction algorithm, the detector quality and the beam divergence

... in reality the image is normally blurred between voxels

X-ray imaging or neutron imaging?

...Depends on what you want to see!



Neutron sources



Institut Laue Langevin, Grenoble, France: Reactor source



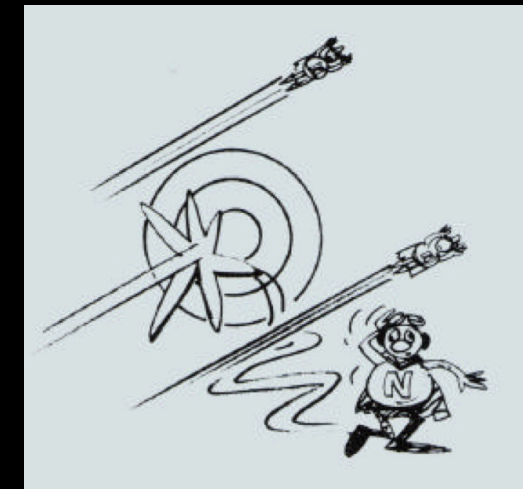
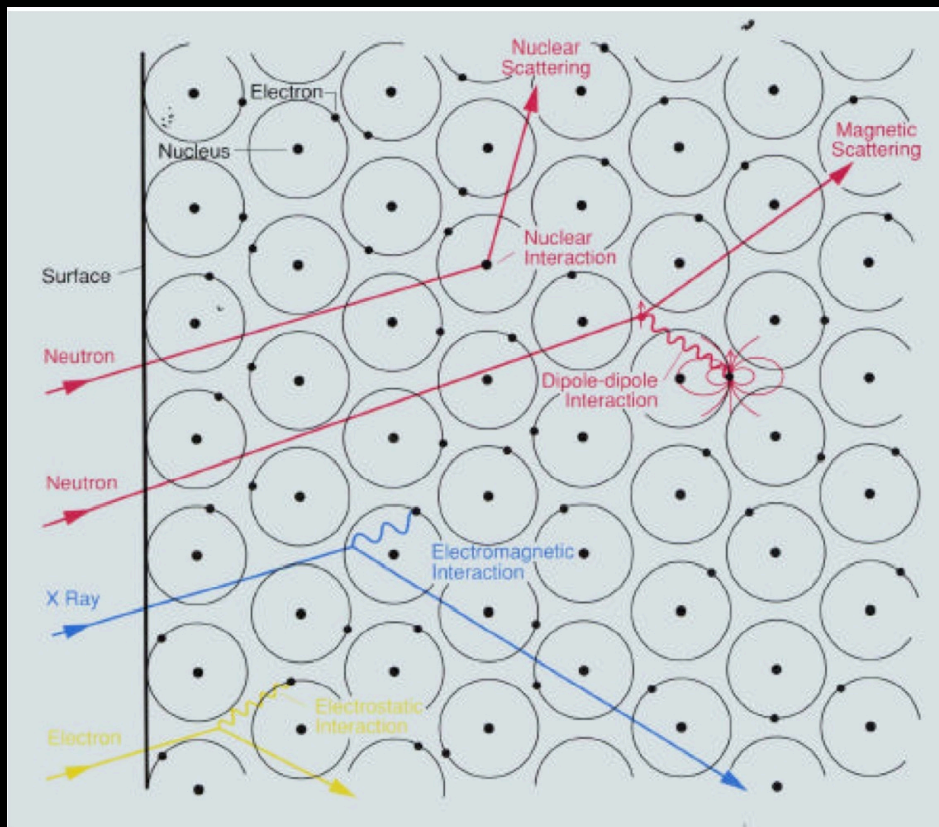
EUROPEAN
SPALLATION
SOURCE



European Spallation Source, Lund, Sweden

Neutron imaging

Neutron interaction mechanisms

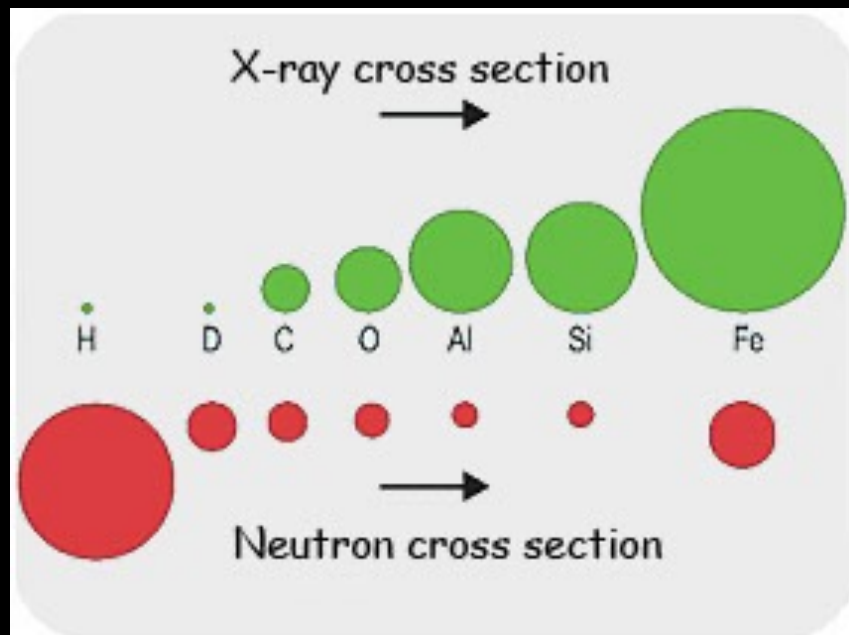


- Neutrons interact with atomic nuclei via very short range ($\sim 10^{-15}\text{m}$) forces.
- Neutrons also interact with unpaired electrons and therefore “see” magnetism.

After R. Pynn (Los Alamos National Laboratory)

X-ray imaging or neutron imaging?

...Depends on what you want to see!



- Different sensitivities
- Different penetration depths for different materials
 - Can see into dense objects with neutrons

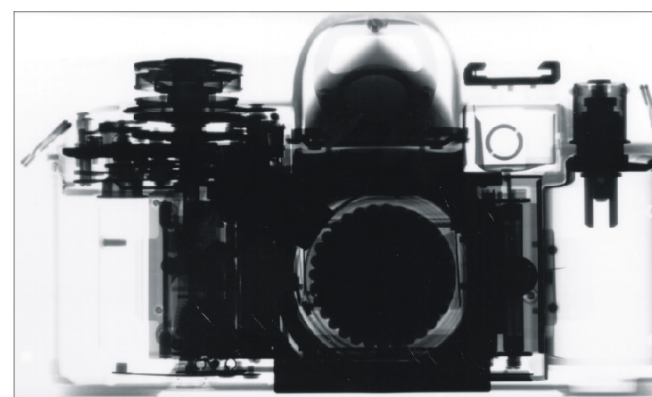


Fig. b: Radiographic image of a camera made X-rays

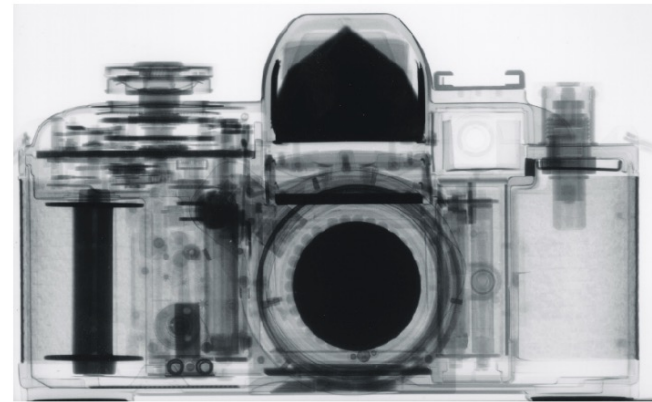


Fig. a: Neutron radiography of a camera

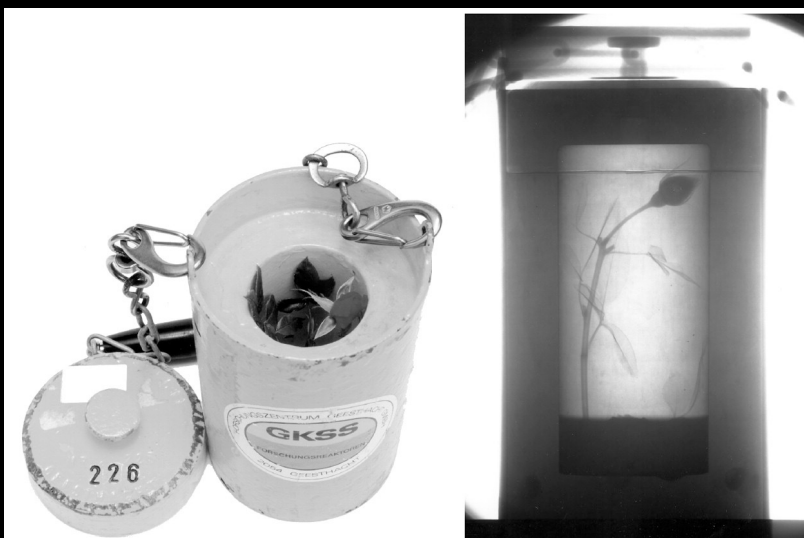
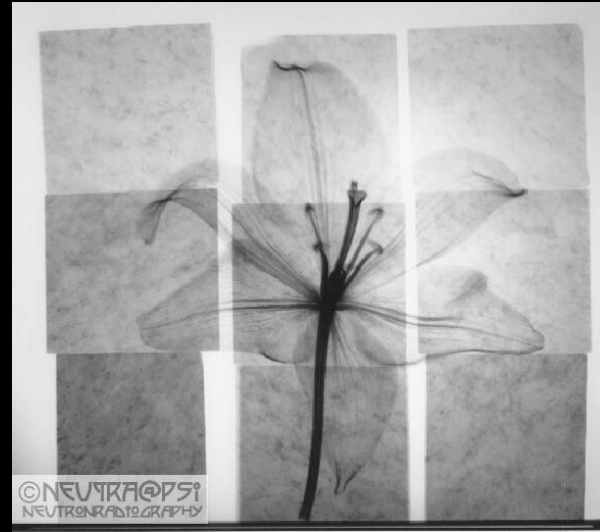
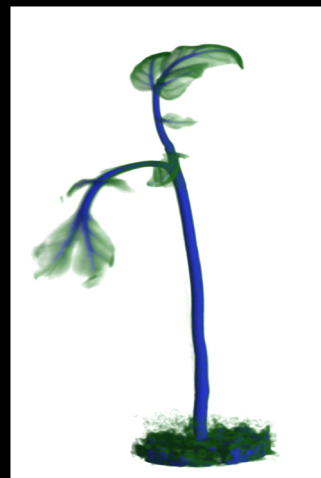
Why use neutrons

Some advantages:

High penetration power

High sensitivity to Hydrogen

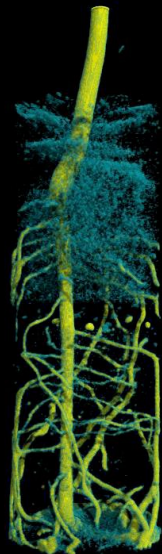
Low radiation damage



Why use neutrons

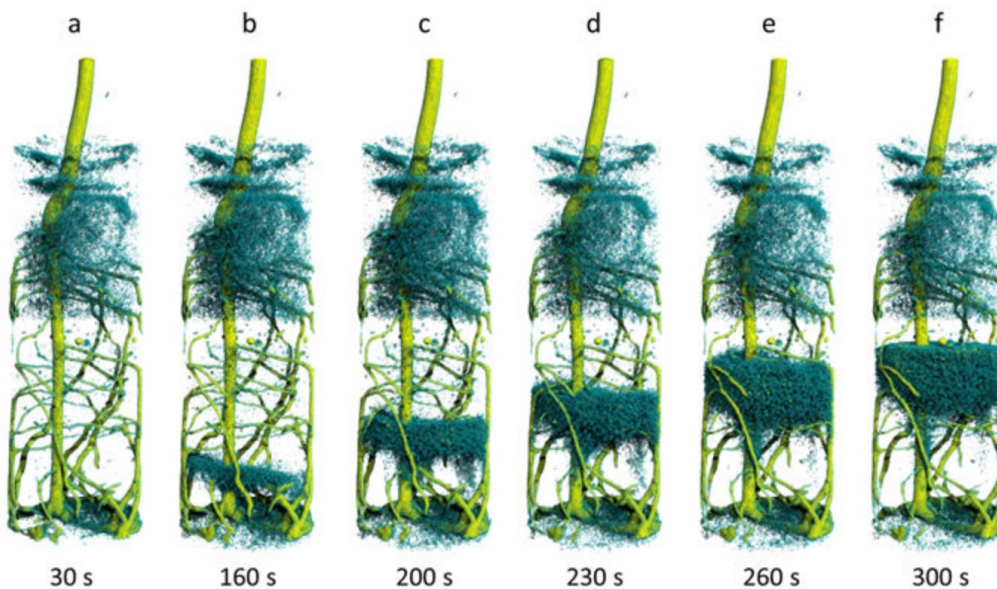
Some advantages:

Isotope sensitivity



time : 0 s

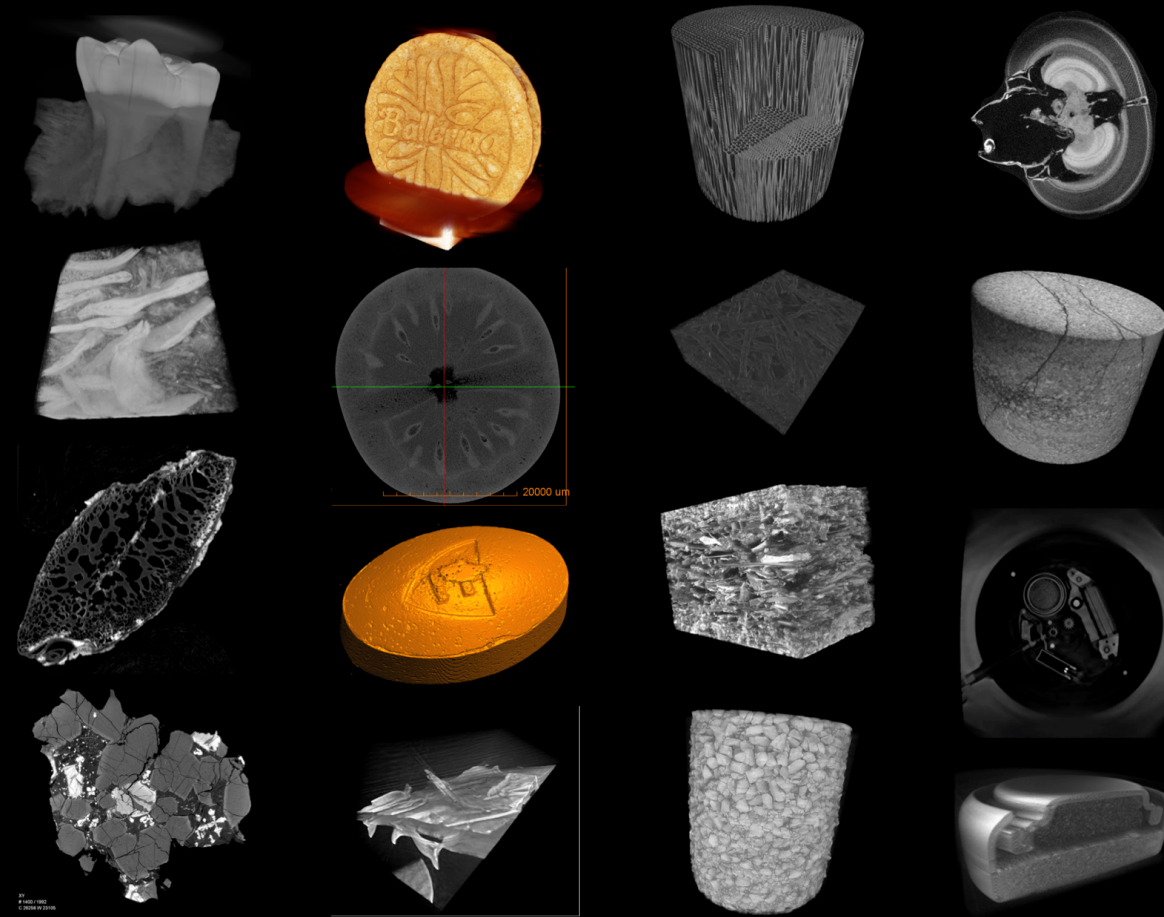
10 mm



Time-resolved neutron tomography of the lupine root system after the injection of 4 ml deuterated water (D_2O) through the bottom. The time series ($30 \text{ s} \leq t \leq 300 \text{ s}$) shows the ascending front of water (H_2O) displaced by deuterated water moving upwards. The time resolution for each tomogram is just 10 s. A video of this sequence is provided in the supplementary information.

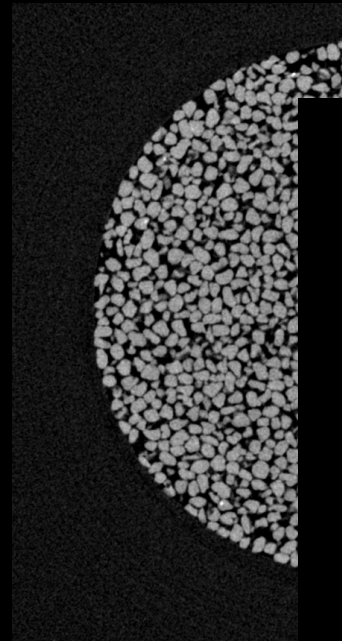
Tötzke et al., Scientific reports, 2017

Multiple applications... and many nice images...

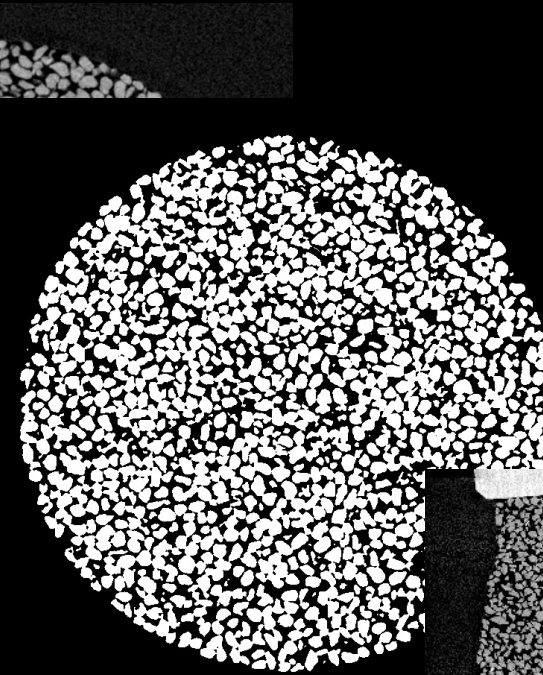


But so what...

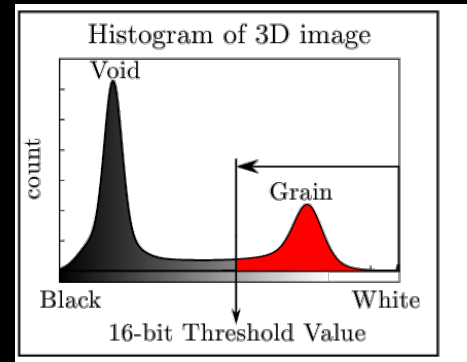
How do we see/identify and characterise microstructure?



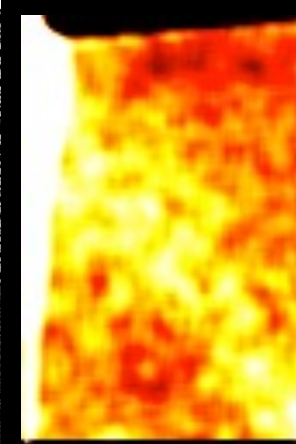
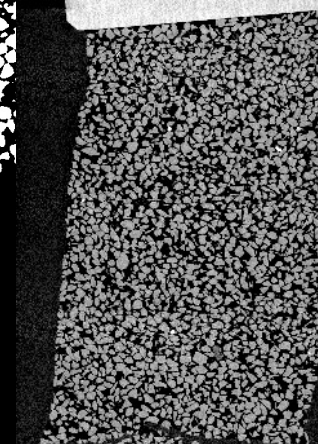
“Raw” image



Binarise
(grains and voids)

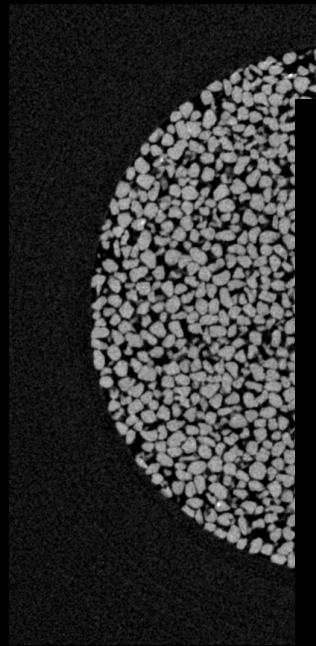


Tomo

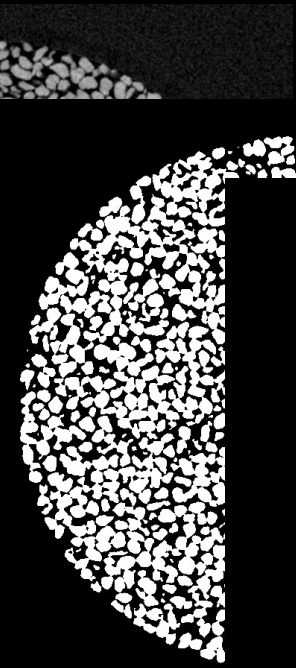


Porosity

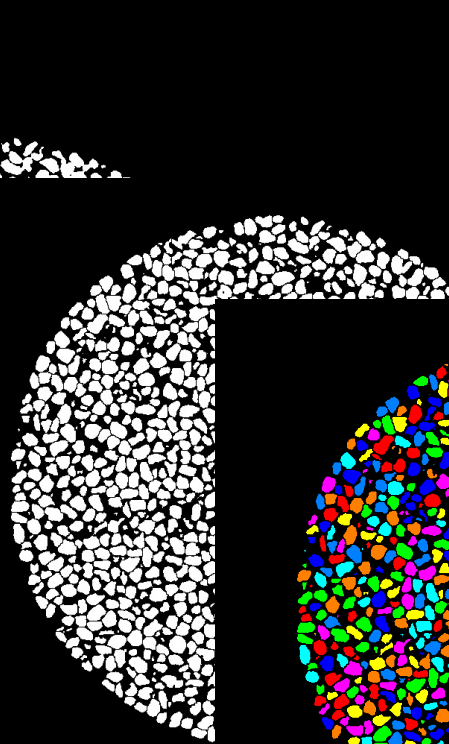
How do we see/identify and characterise microstructure?



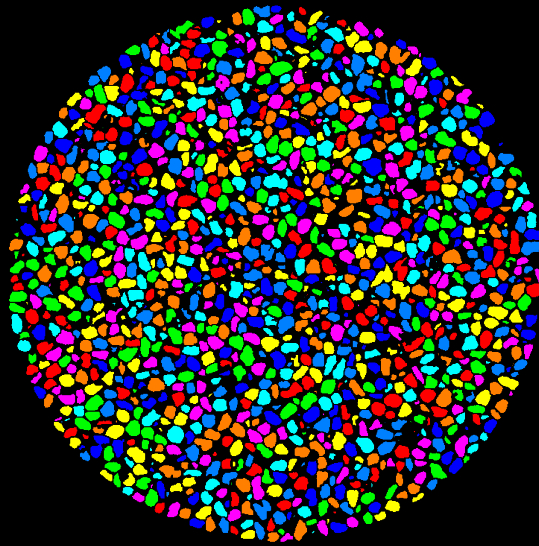
“Raw” image



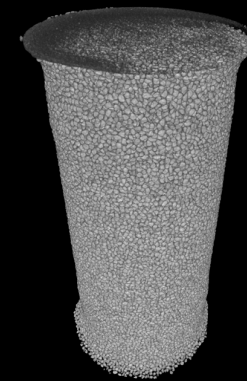
Binarise
(grains and voids)



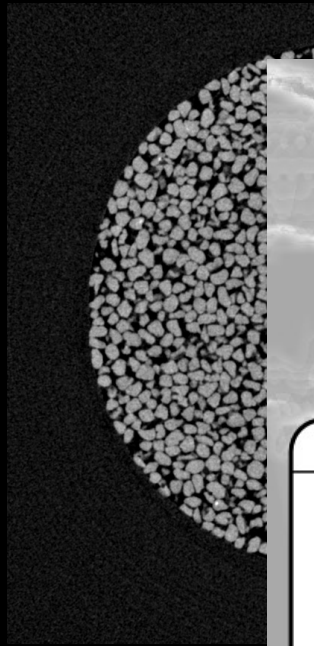
Watershed
Segmentation
(split grains apart)



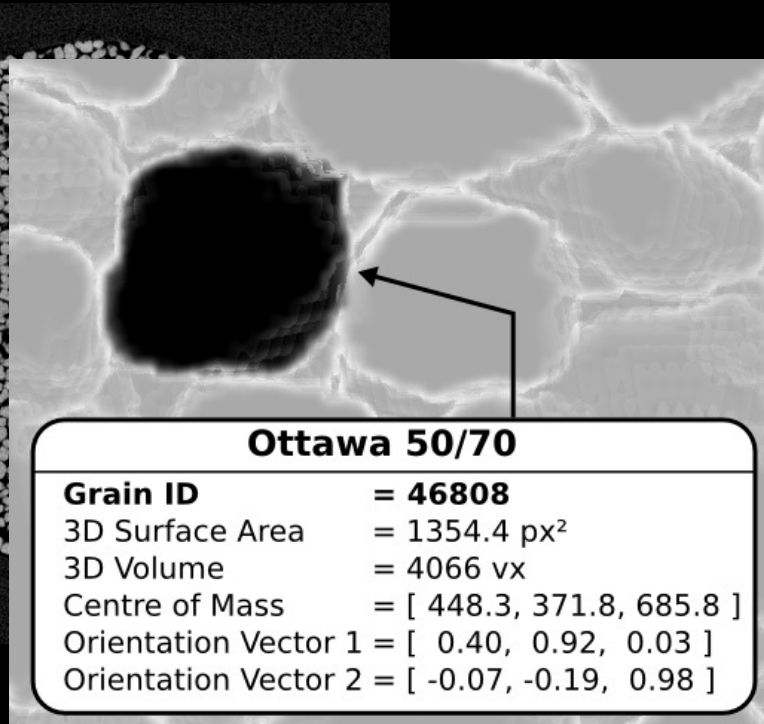
Label Individual Grains



How do we see/identify and characterise microstructure?



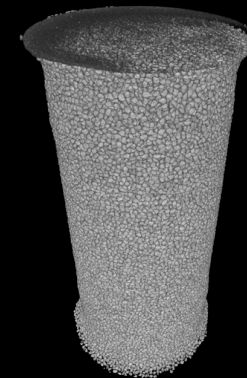
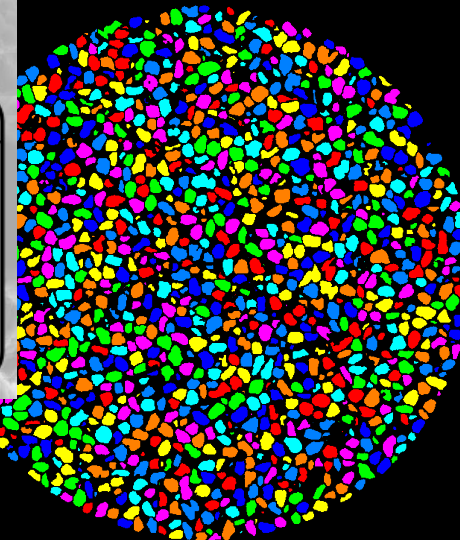
“Raw” image



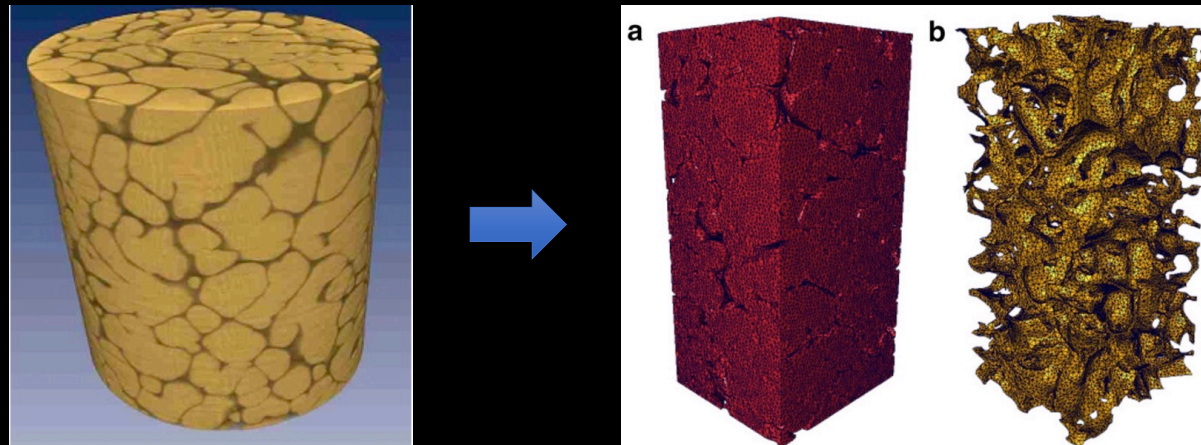
Binarise
(grains and voids)

Watershed
Segmentation
(split grains apart)

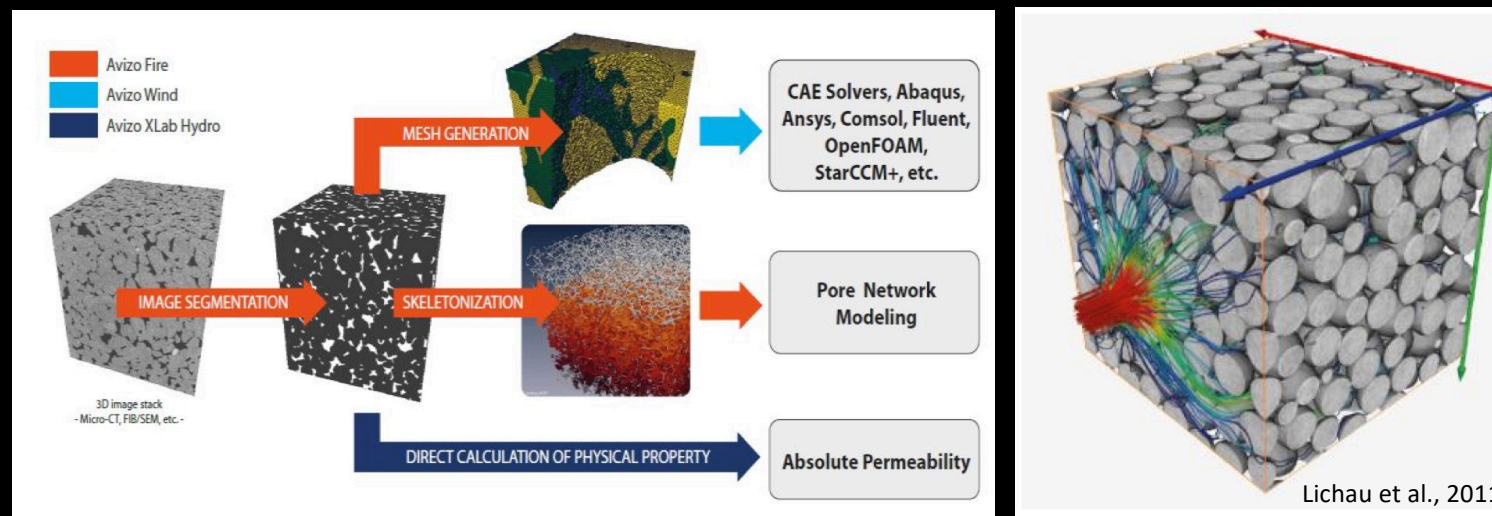
Label Individual Grains



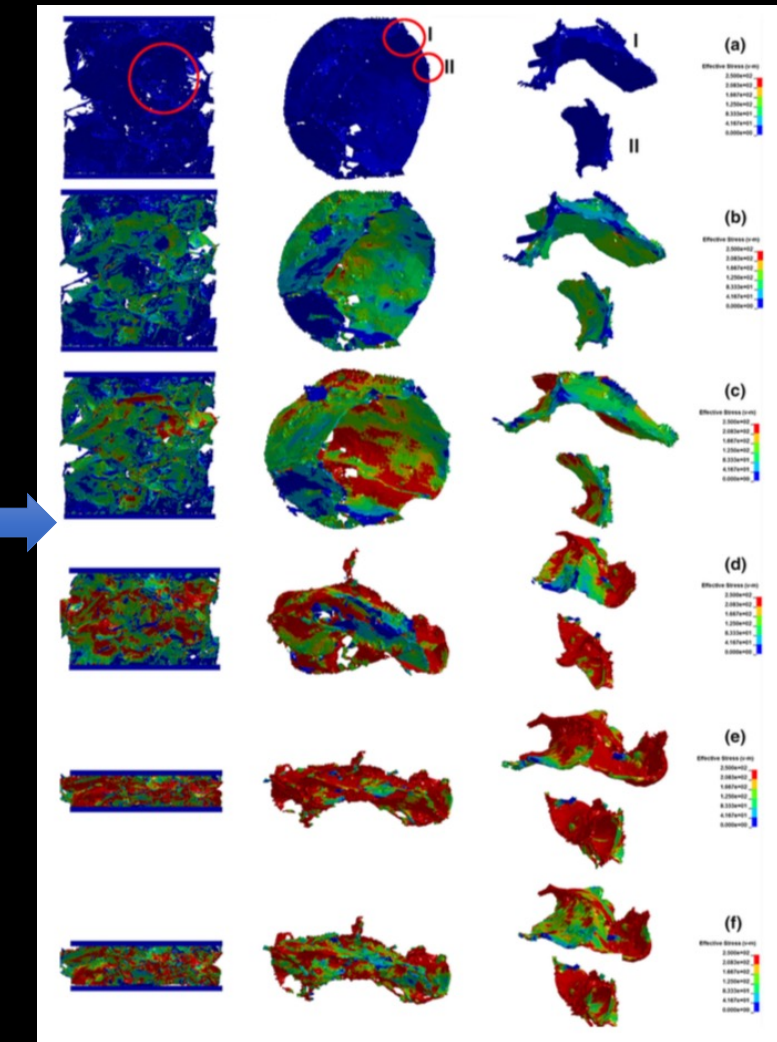
Structural imaging and characterisation → models



Madi et al., 2006



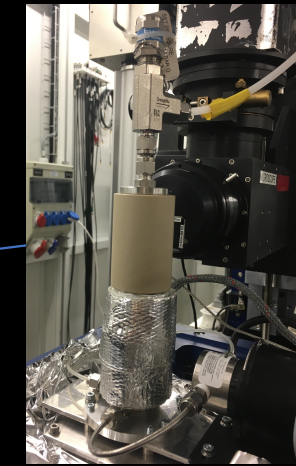
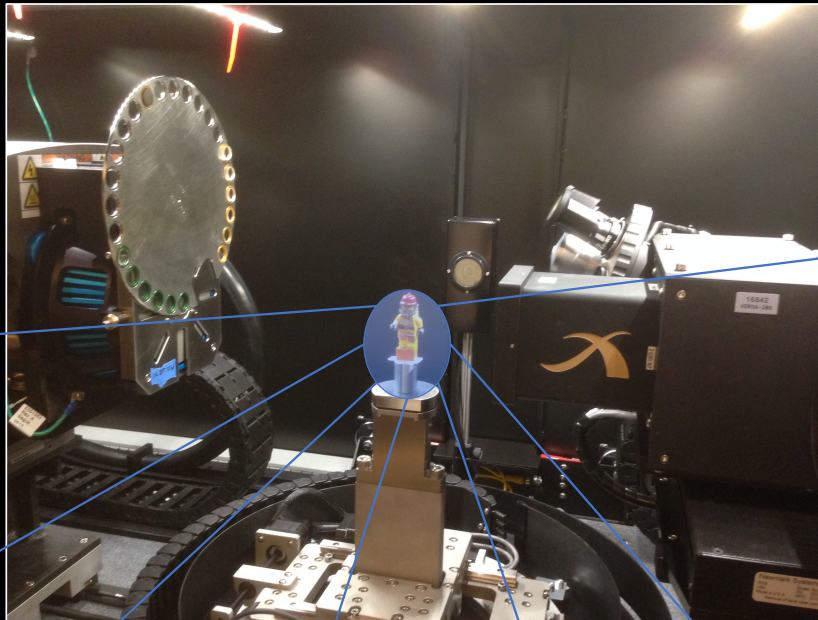
Structural imaging and characterisation → models



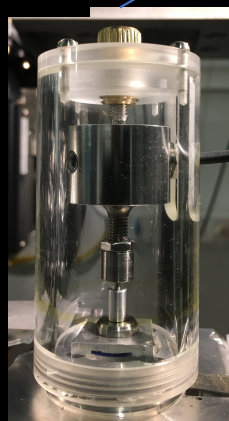
Srinivasa, Kulachenko , Karlberg, 2017, Cellulose

4D imaging...

- In-situ devices



Chemical treatment
(Delignification)



Compression



Tension



Peeling



Vacuum



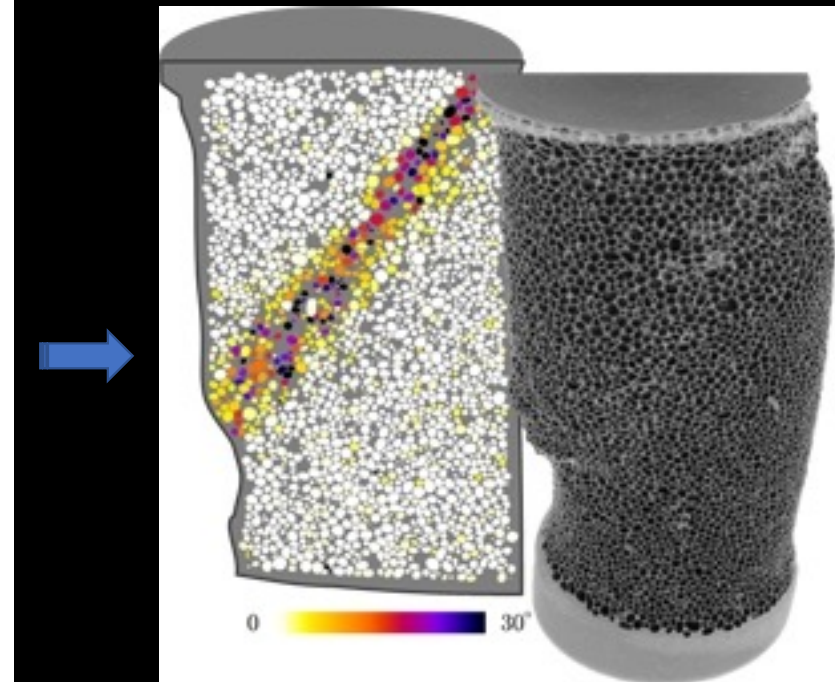
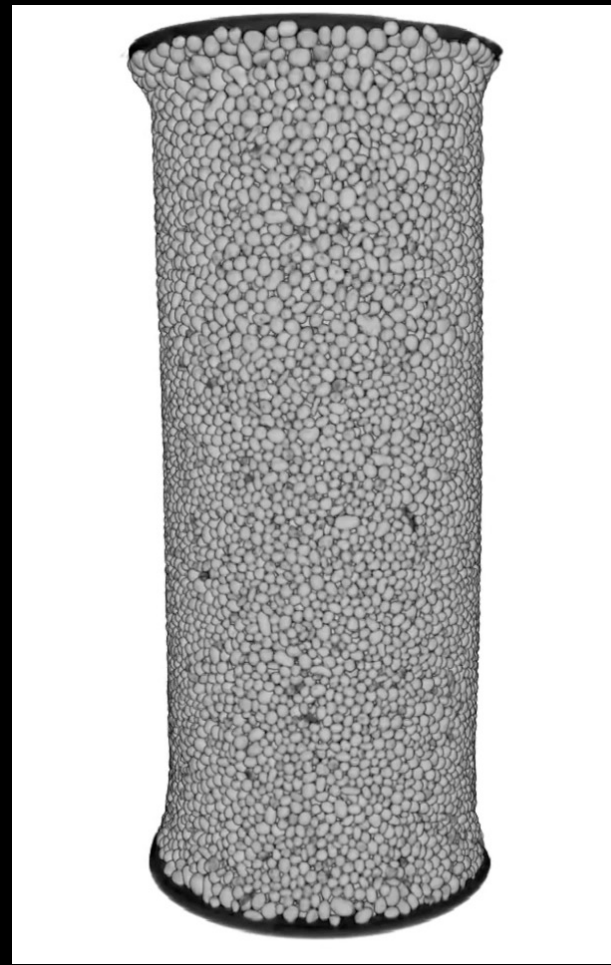
Humidity

Others and Future:

- Pressure
- Fluid flow
- Electrochemical
- Heating
- Cooling (freezing)
- ...

4D imaging and in-situ experiments

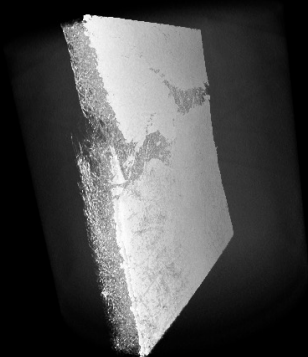
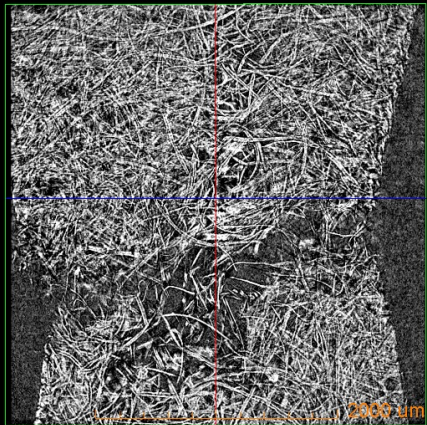
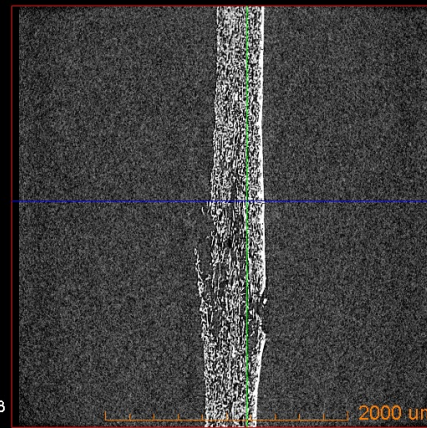
4D imaging of triaxial compression
of a sample of (oolitic) sand
(10's thousands grains)



Quantification of grain kinematics

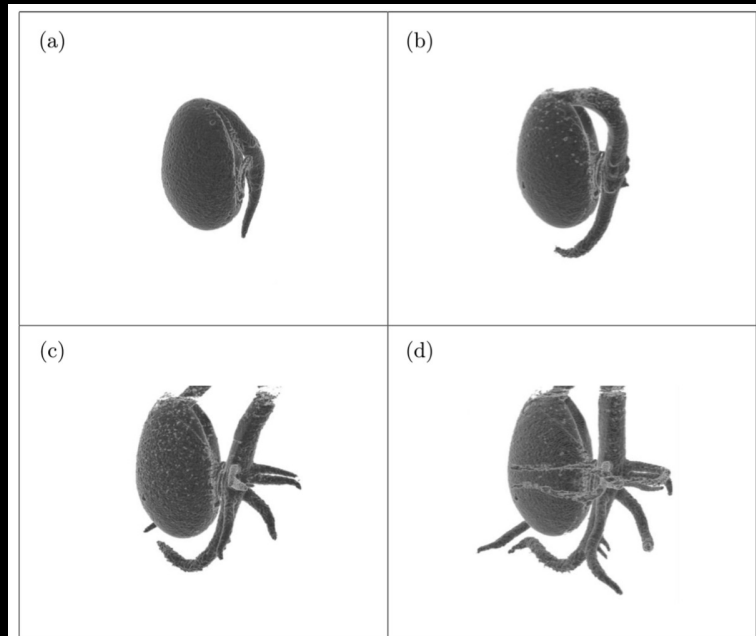
4D imaging and in-situ experiments

“in-situ” tensile testing of paperboard

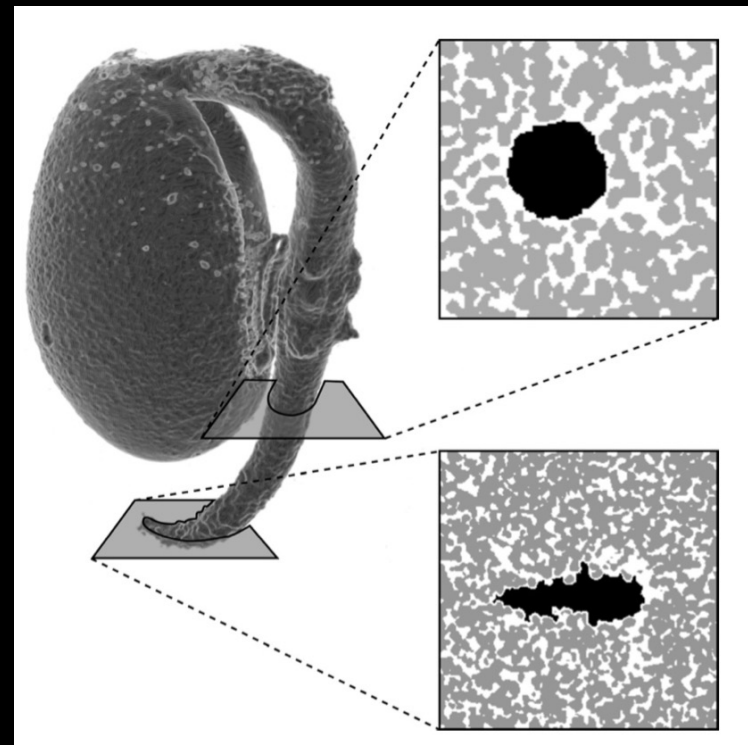


4D imaging and in-situ experiments

Growth of seeds in soil...

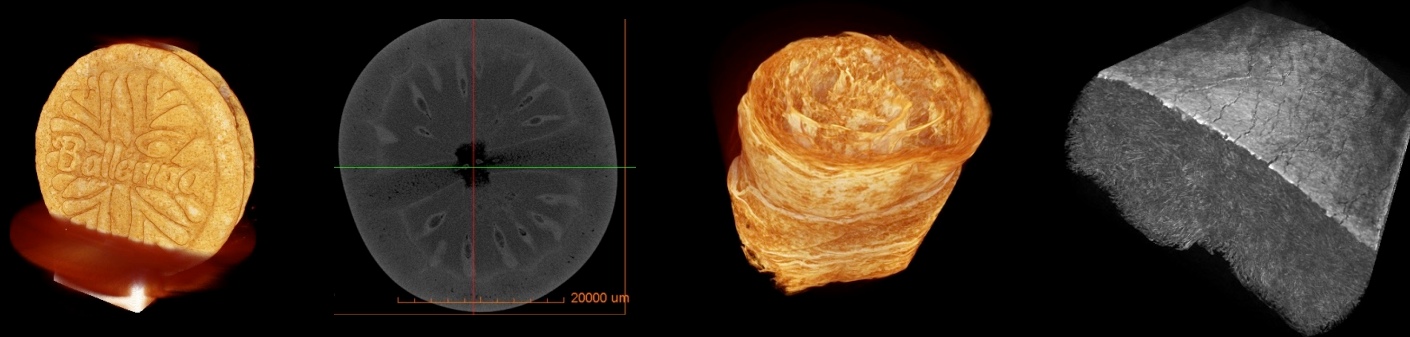


Bean-root system: evolution during germination
(a) 4 days, (b) 5 days, (c) 6 days, and (d) 7 days
after wetting

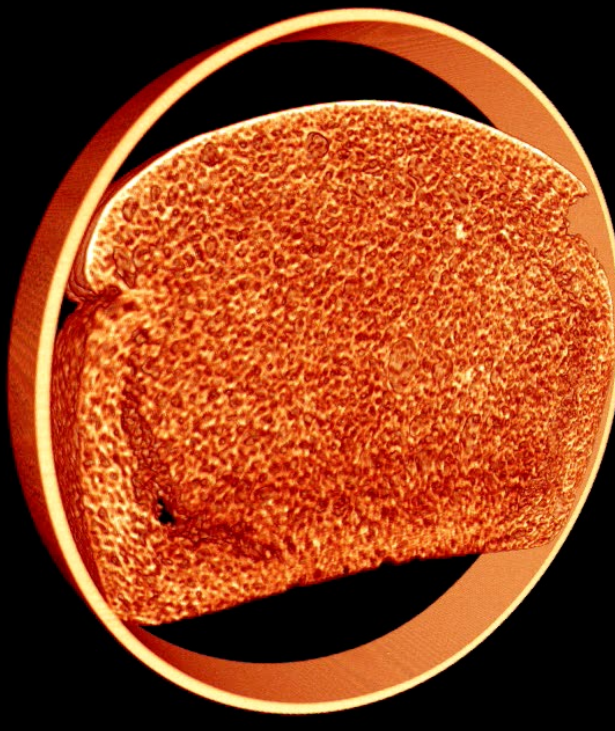


Viggiani et al., 2015

IMAGING FOOD AND PACKAGING

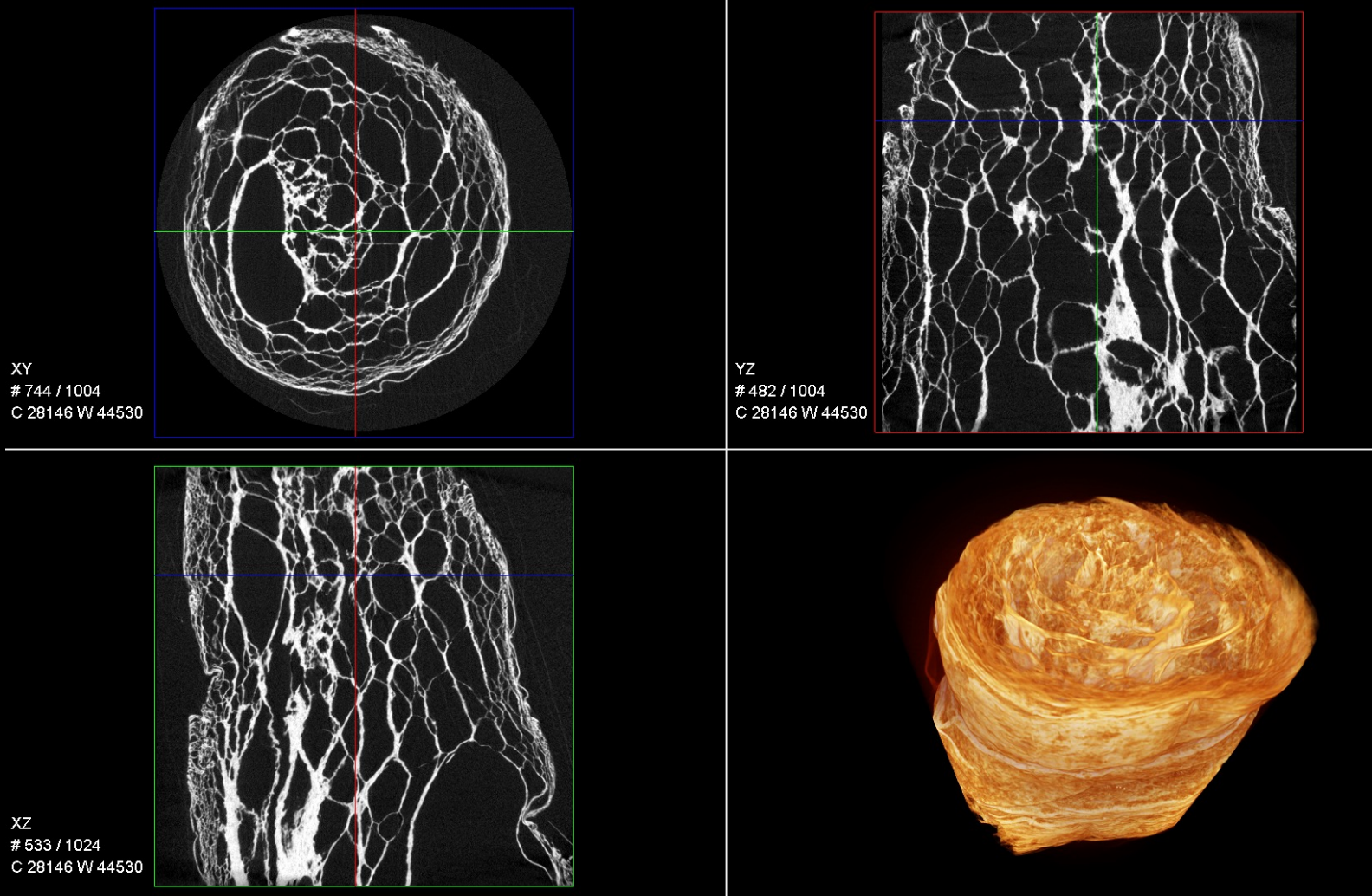


Imaging internal structures: bread-products



← →
≈ 25 mm

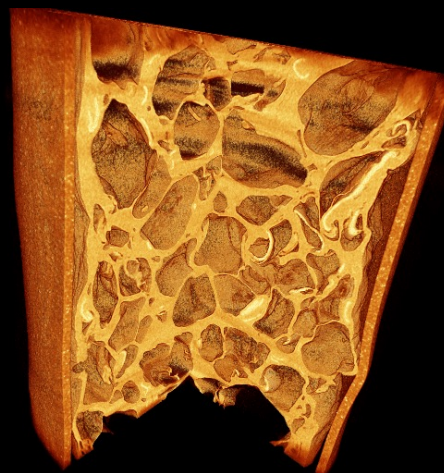
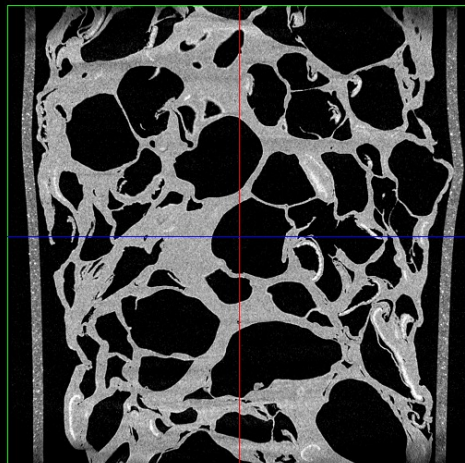
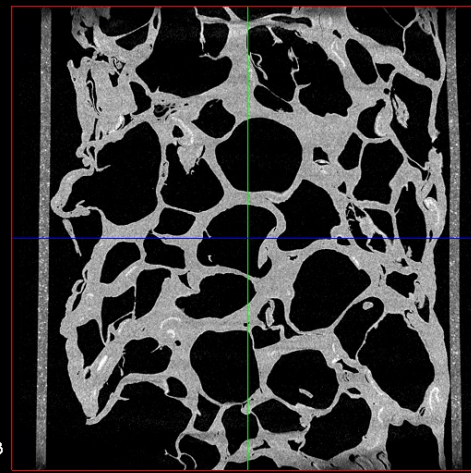
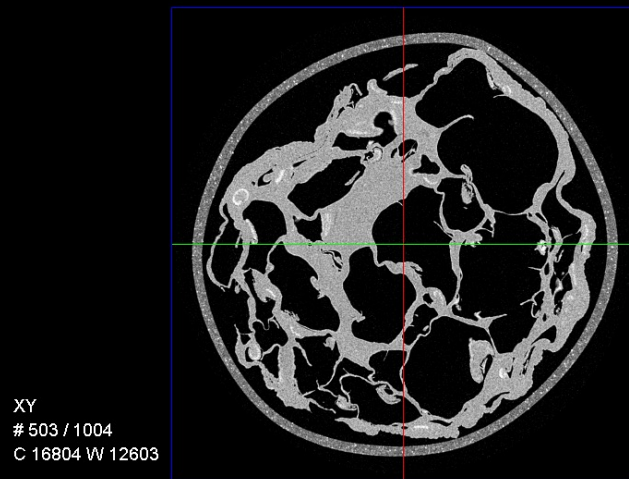
Imaging internal structures: bread-products



Collab. N. Lorén, RISE

4D IMAGING LAB@LTH

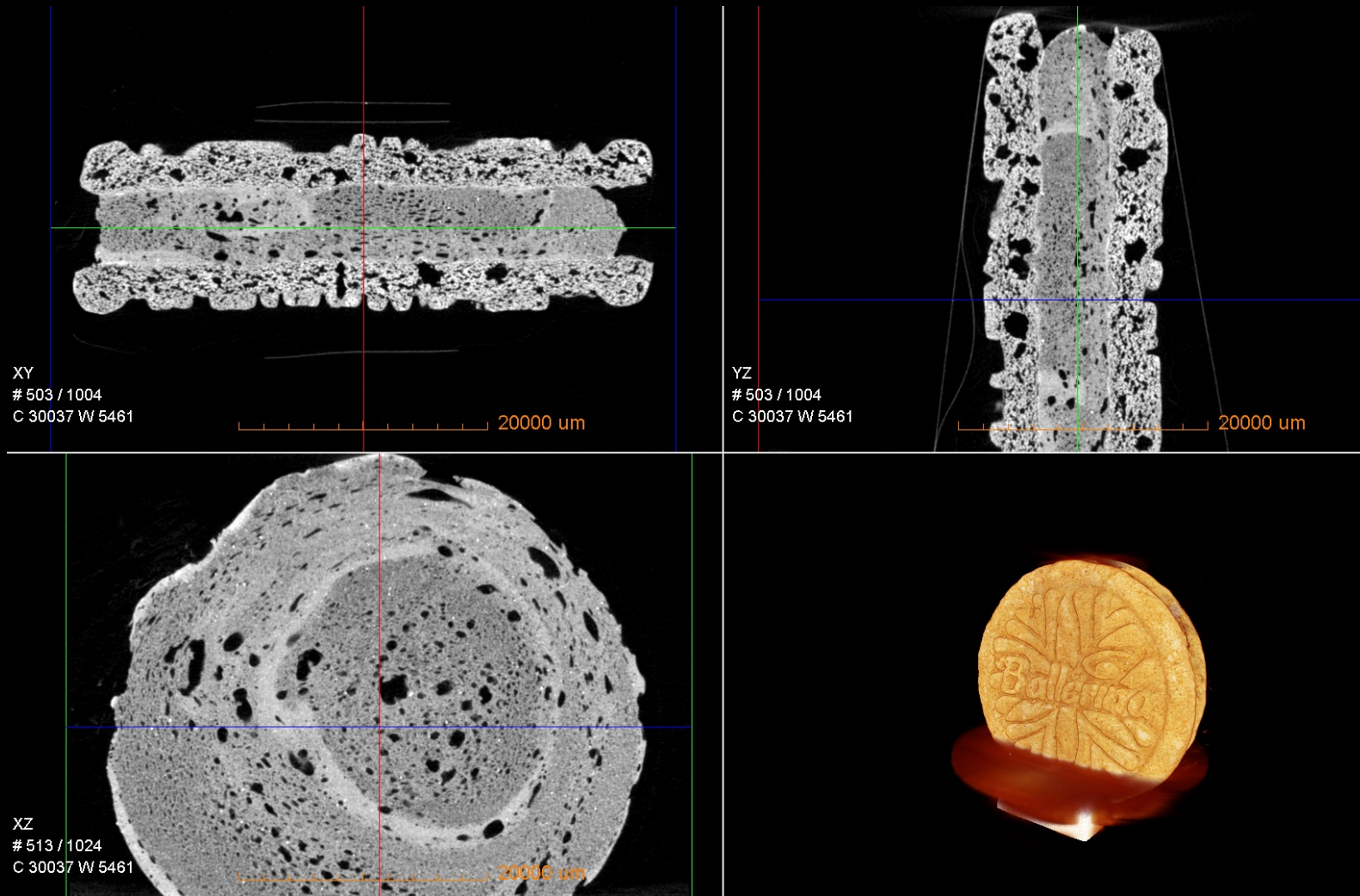
Extruded product structure



Collab. N. Lorén, RISE

4D IMAGING LAB@LTH

Imaging internal structures: biscuit-filling interaction



Collab. N. Lorén, RISE

4D IMAGING LAB@LTH

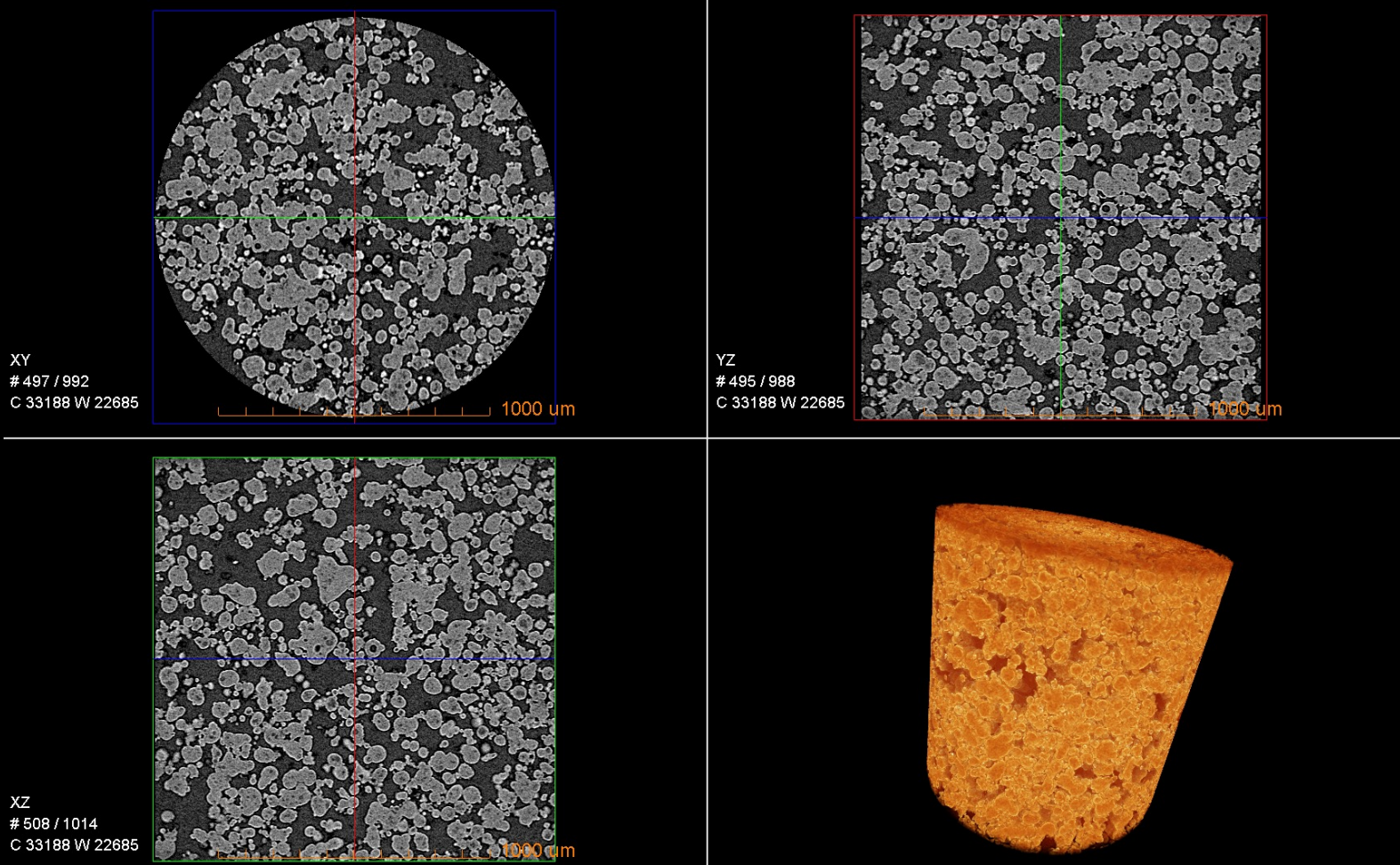
Imaging internal structures: biscuit-filling interaction



Collab. N. Lorén, RISE

[4D IMAGING LAB@LTH](#)

Whole-milk powder structure



Collab. B. Bergenstahl, Food Tech, LTH

4D IMAGING LAB@LTH

Freeze-dried milk powder structure

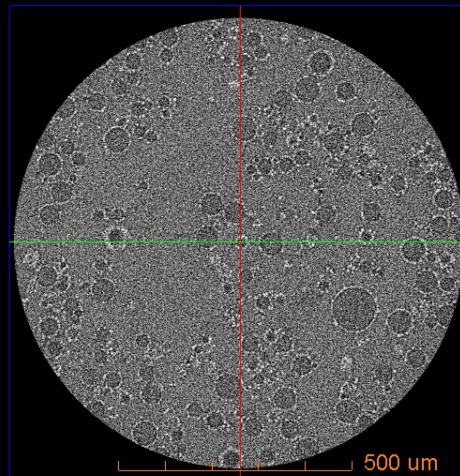


FoV = 324 μm

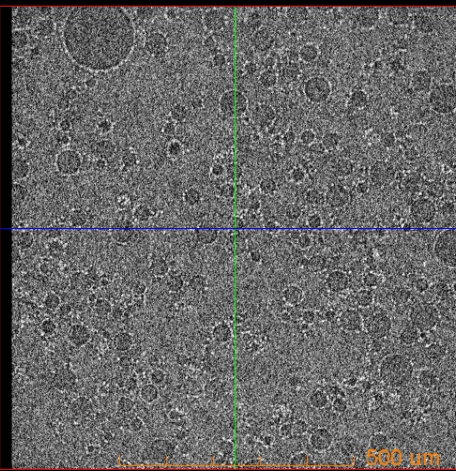
4D IMAGING LAB@LTH

Pickering emulsions (rice based)

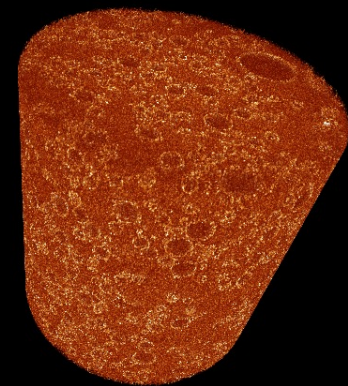
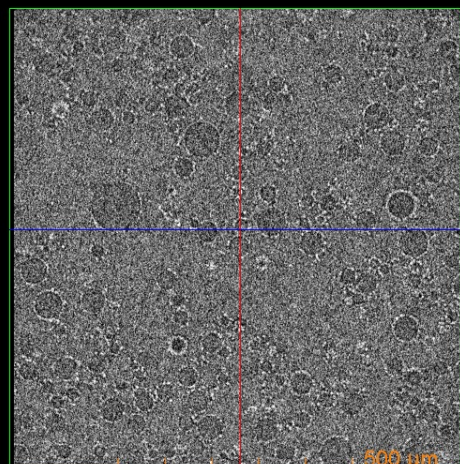
XY
514 / 988
C 15334 W 10502



YZ
494 / 964
C 15334 W 10502



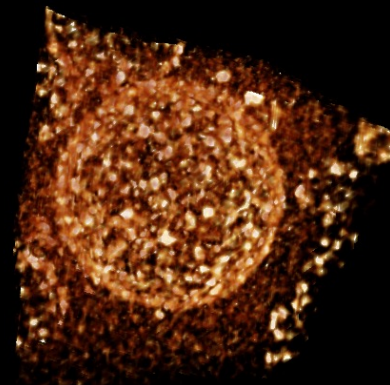
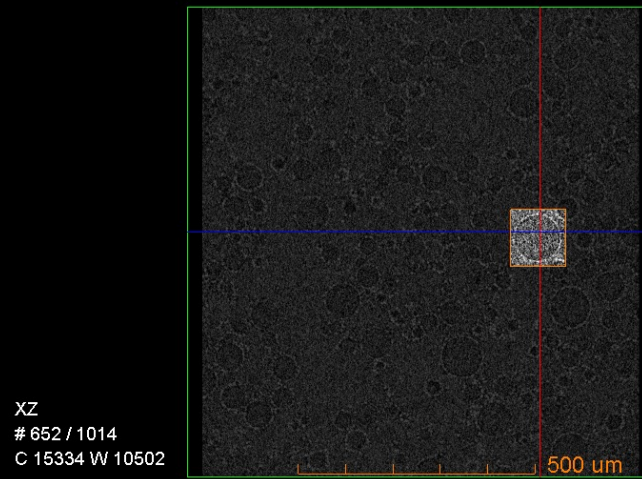
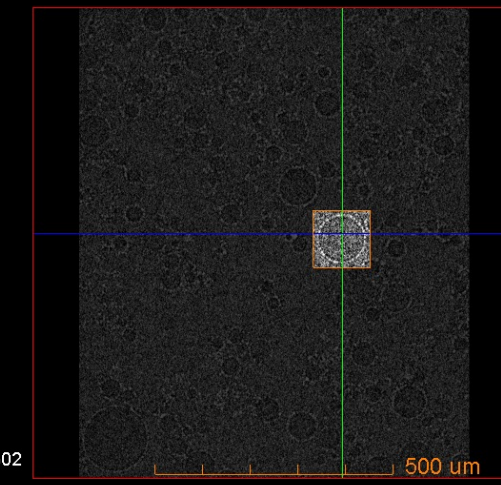
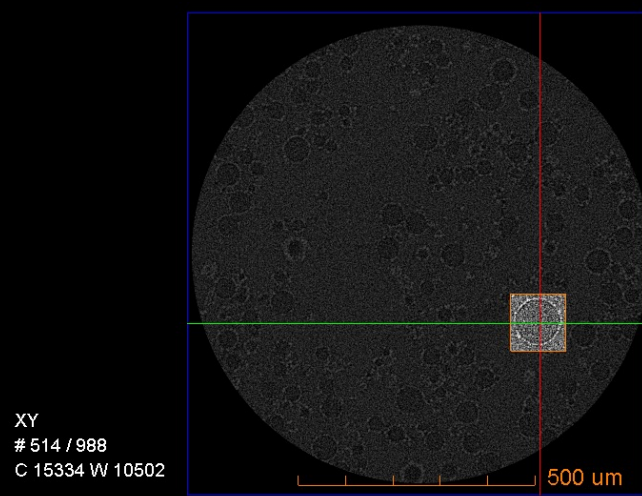
XZ
504 / 1014
C 15334 W 10502



Collab. M. Rayner, Food Tech. LTH

4D IMAGING LAB@LTH

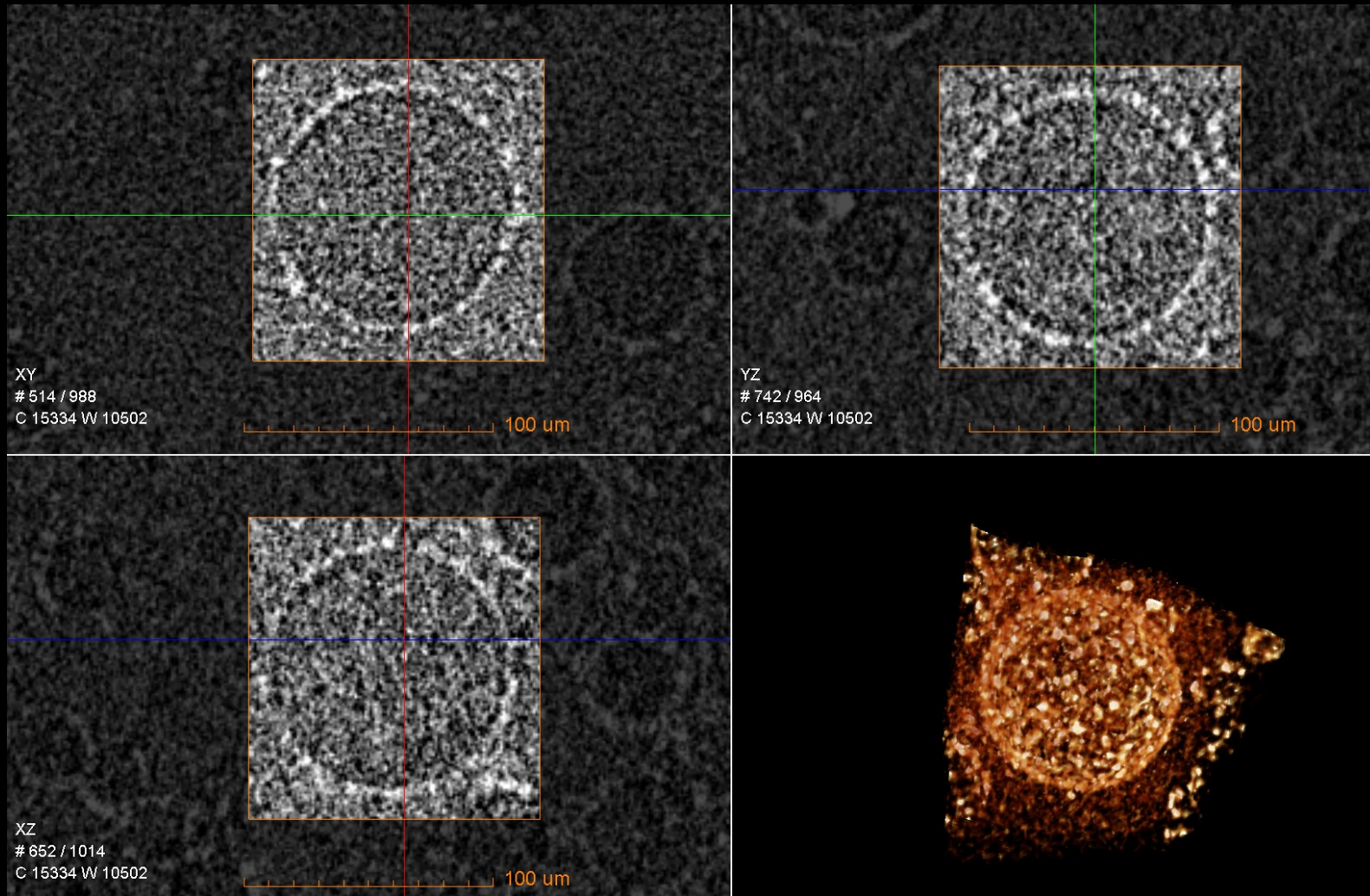
Pickering emulsions (rice based)



Collab. M. Rayner, Food Tech. LTH

4D IMAGING LAB@LTH

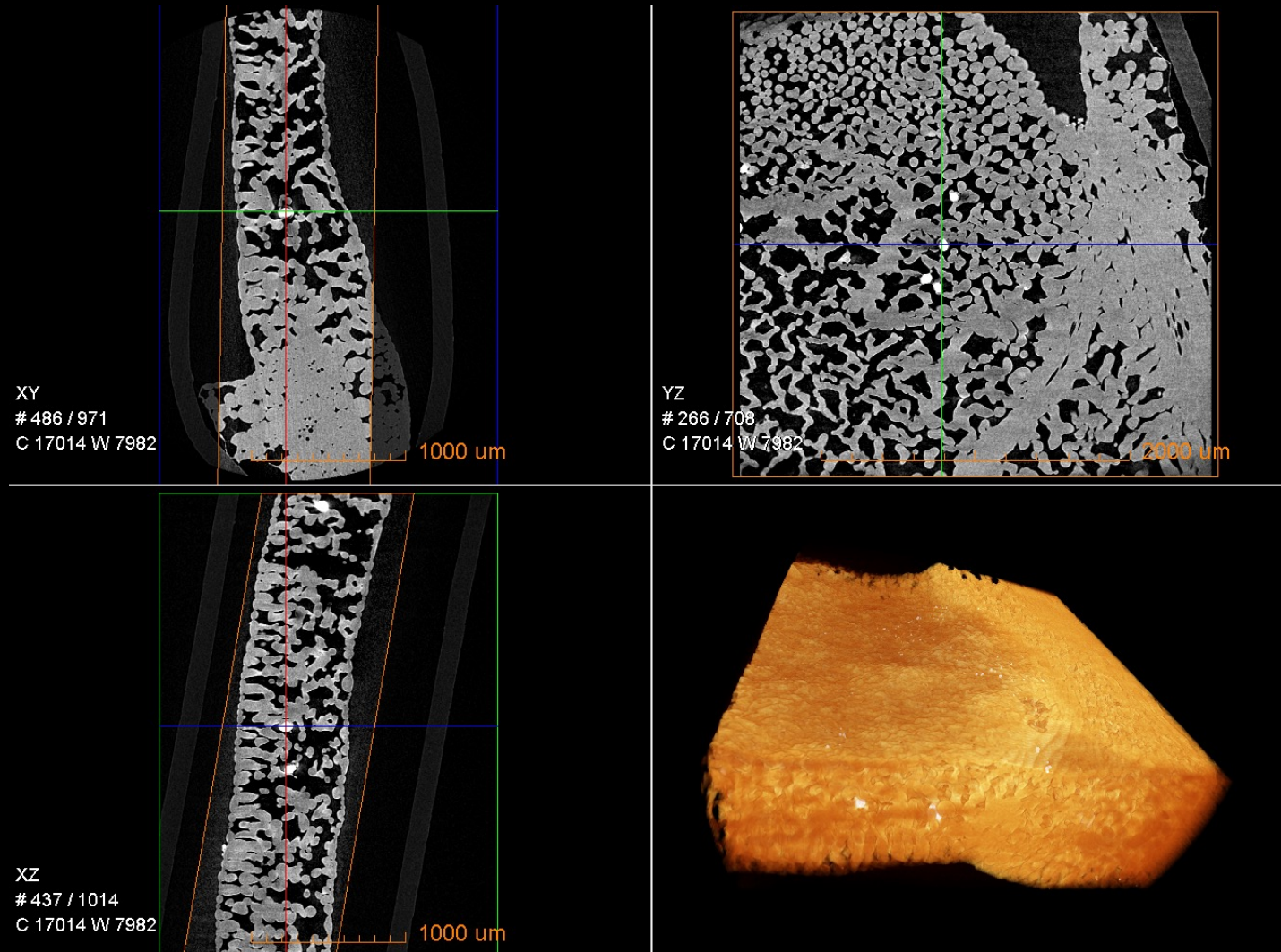
Pickering emulsions (rice based)



Collab. M. Rayner, Food Tech. LTH

4D IMAGING LAB@LTH

Internal structure of leaves towards optimisation of processing (freezing ,drying...)



Collab. F. Gomez & N.L. Yousef, Food Tech., LTH

4D IMAGING LAB@LTH

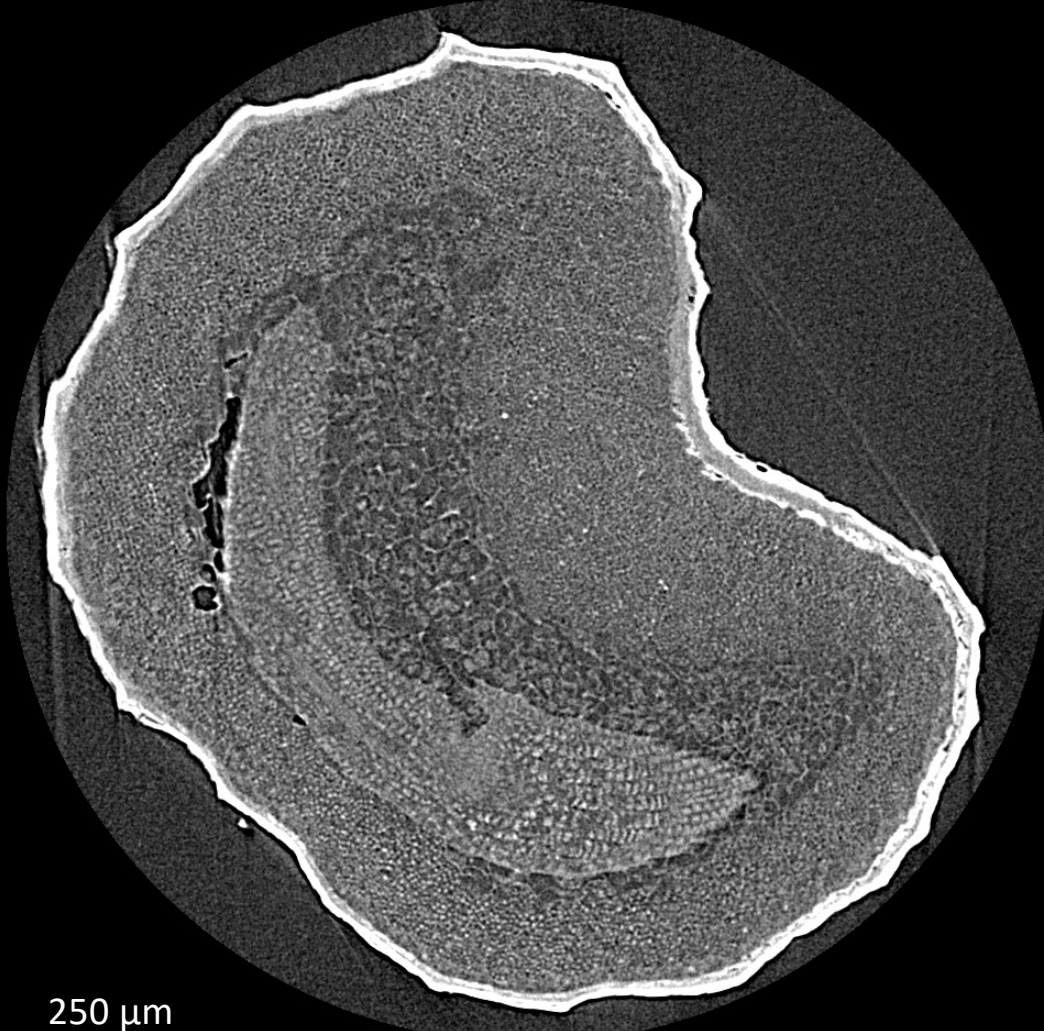
Internal structure of soft fruits/berries



Collab. N. Lorén, RISE

4D IMAGING LAB@LTH

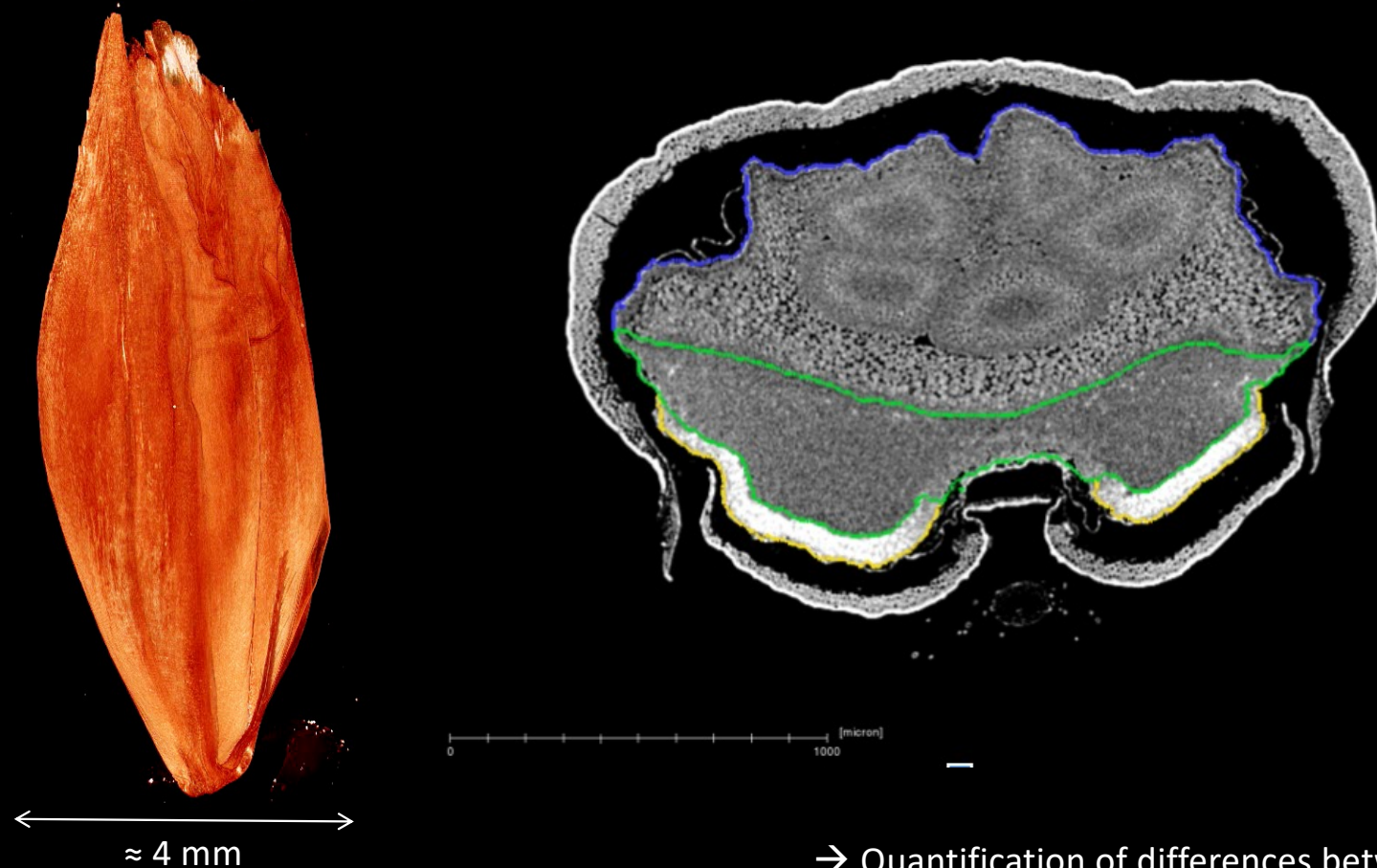
Seeds: Internal structure of a poppy seed



250 μm

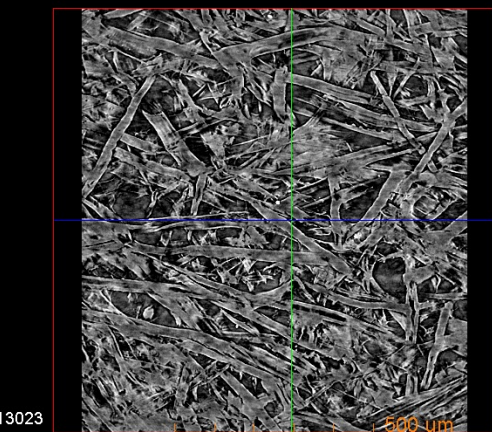
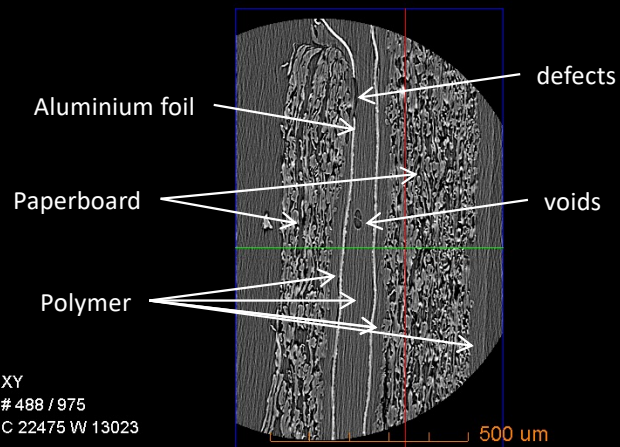
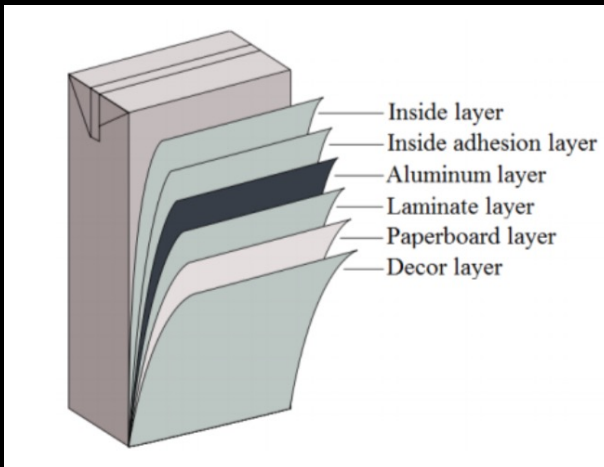
NG LAB@LTH

Seeds: Analysis of structures in barley and oat mutants

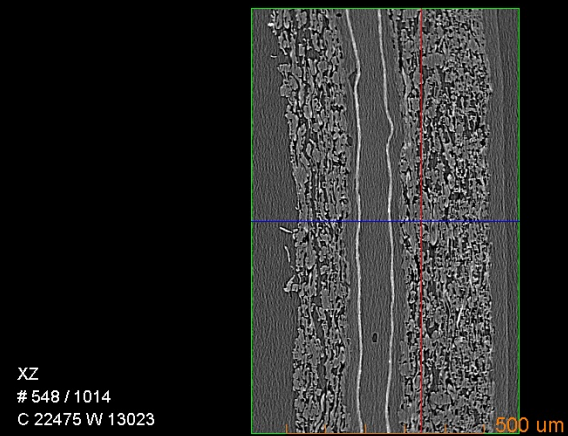


→ Quantification of differences between cereal mutations

Imaging of packaging materials

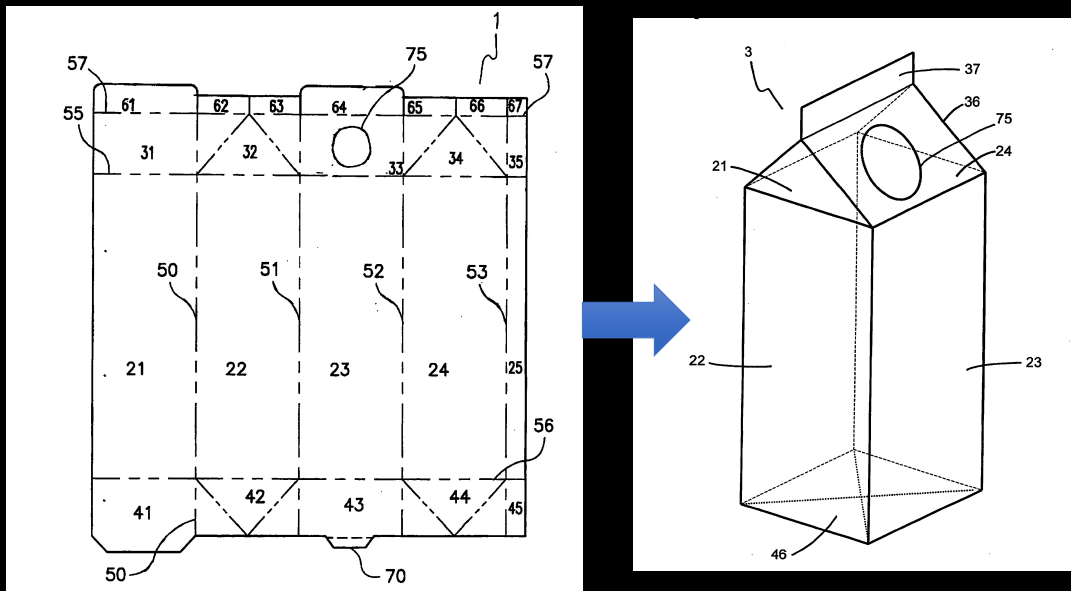


TetraPak recart



Packaging production

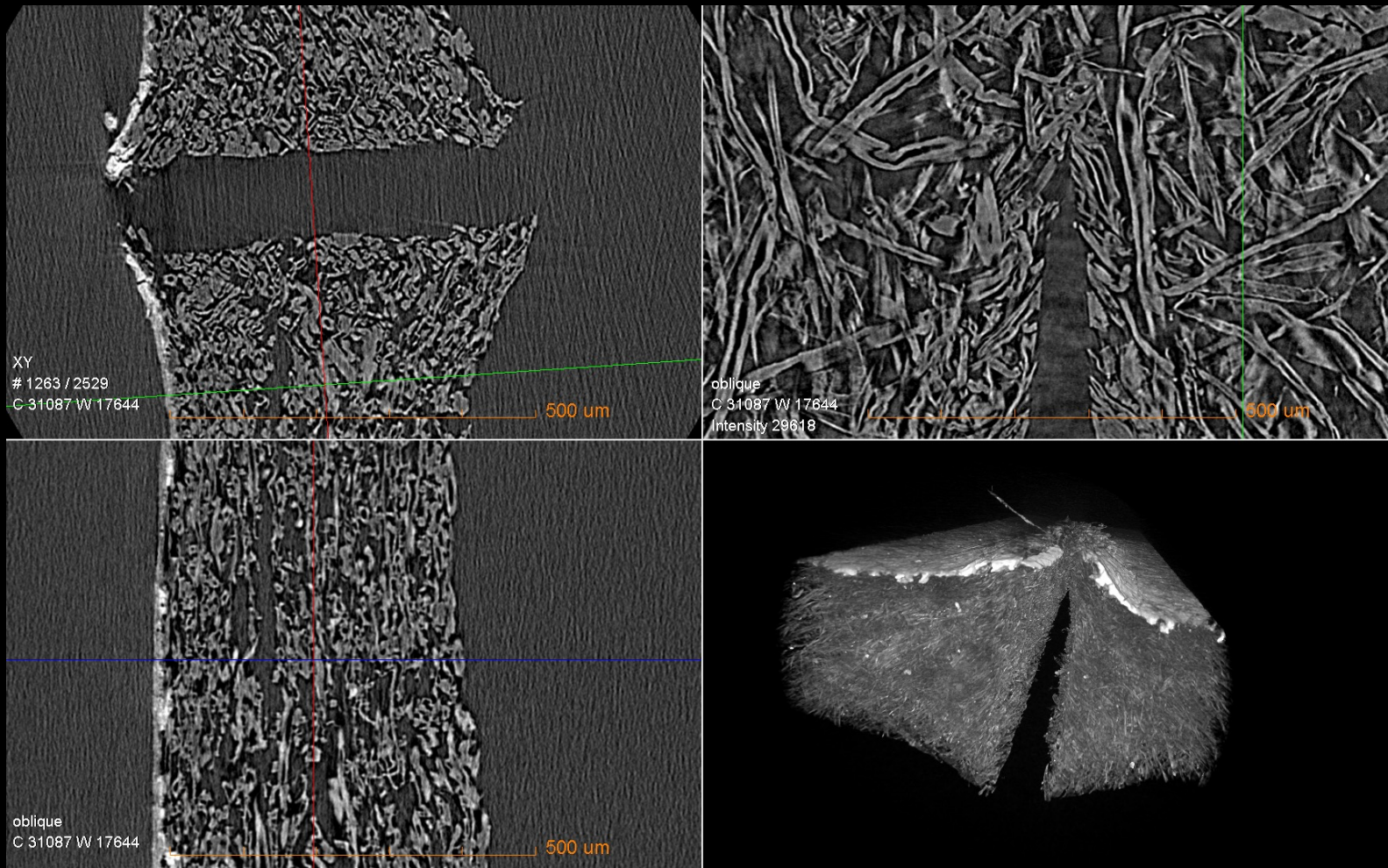
Paperboard package production involves a number of processing steps, including creasing and folding that produce significant deformation of the material...



... What happens to the material(s) during these processes?
... How can the processes be optimised to mitigate product failure?

→ 3D imaging can be used to investigate material structure, deformation and process mechanisms

Sharp edge cutting through paperboard

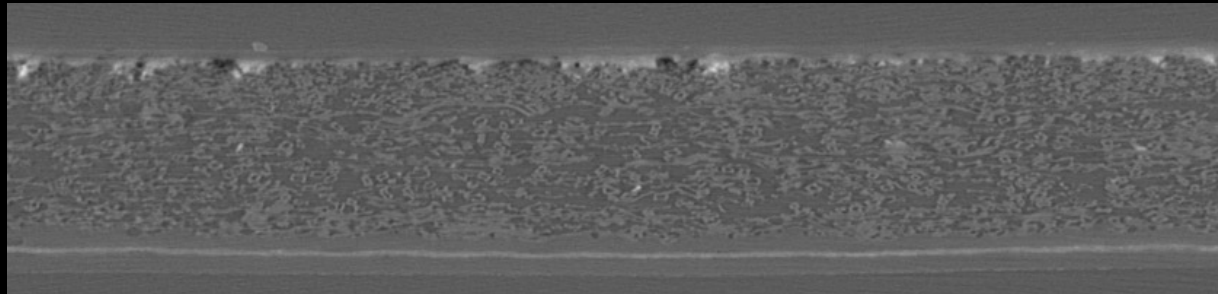


Leek & Jern, MSc Thesis, Div. Solid Mechanics, LTH In Collaboration with TetraPak

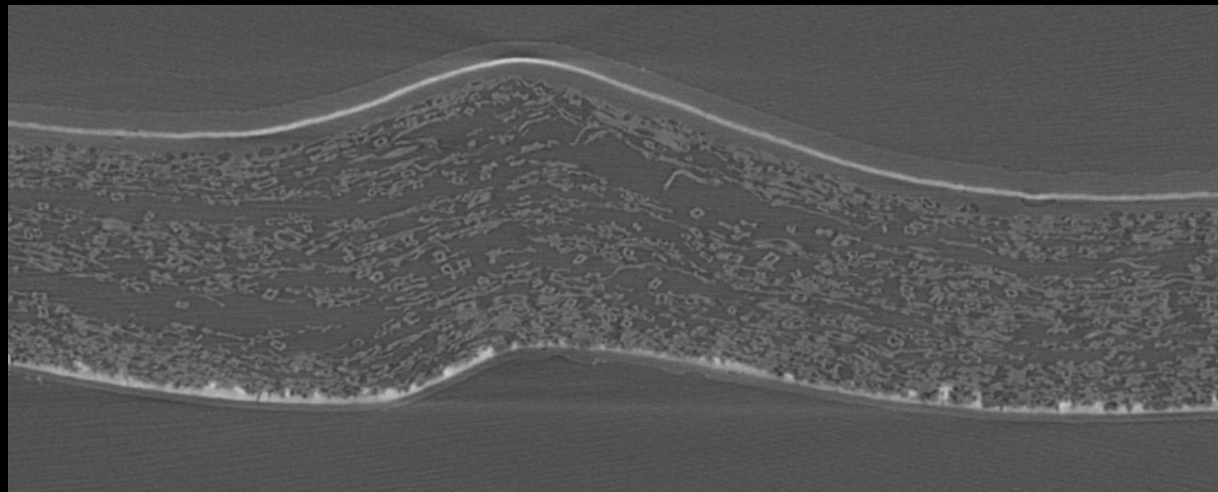
4D IMAGING LAB@LTH

Deformation due to folding

“non-deformed” material

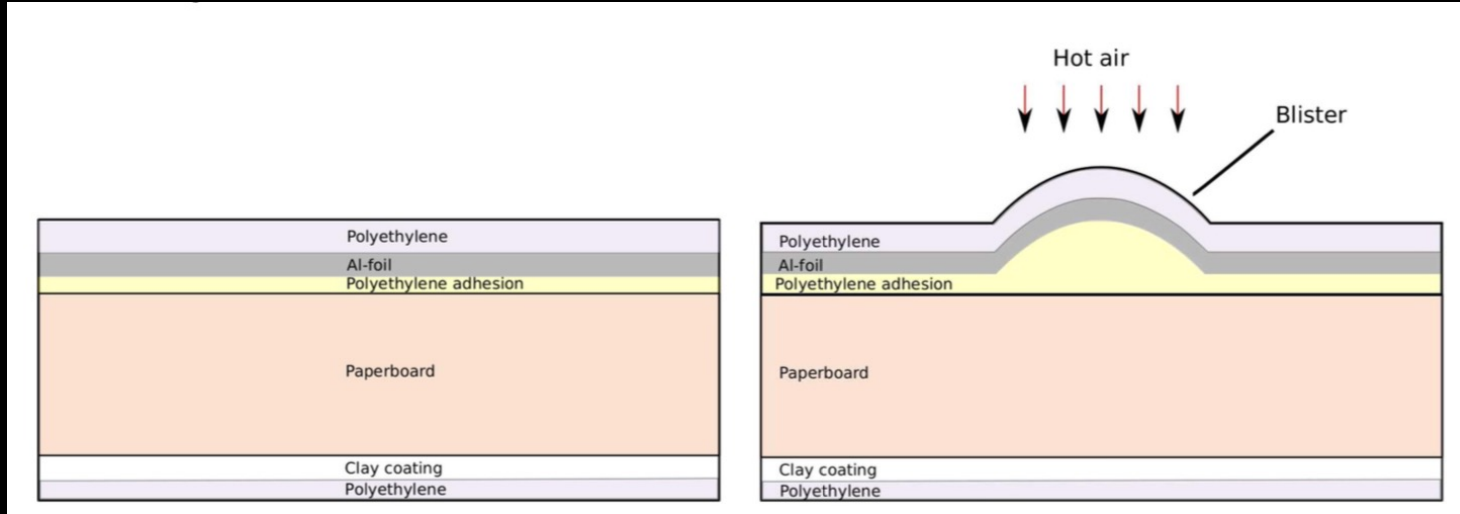


Corner fold



4D IMAGING LAB@LTH

Blistering & Wrinkling in Paperboard



Askfelt & Ristinmaa, 2017

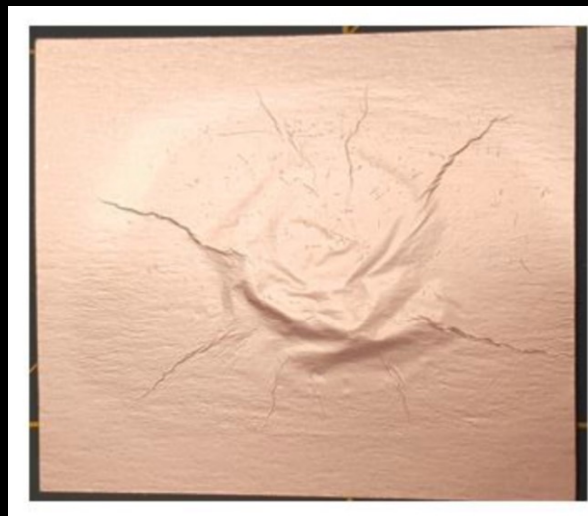
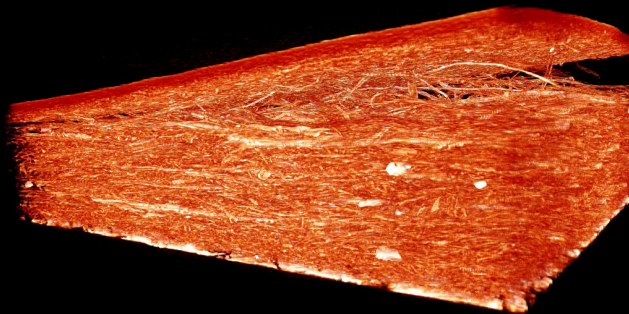
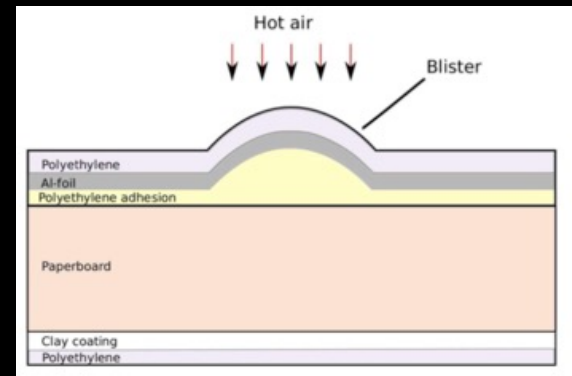
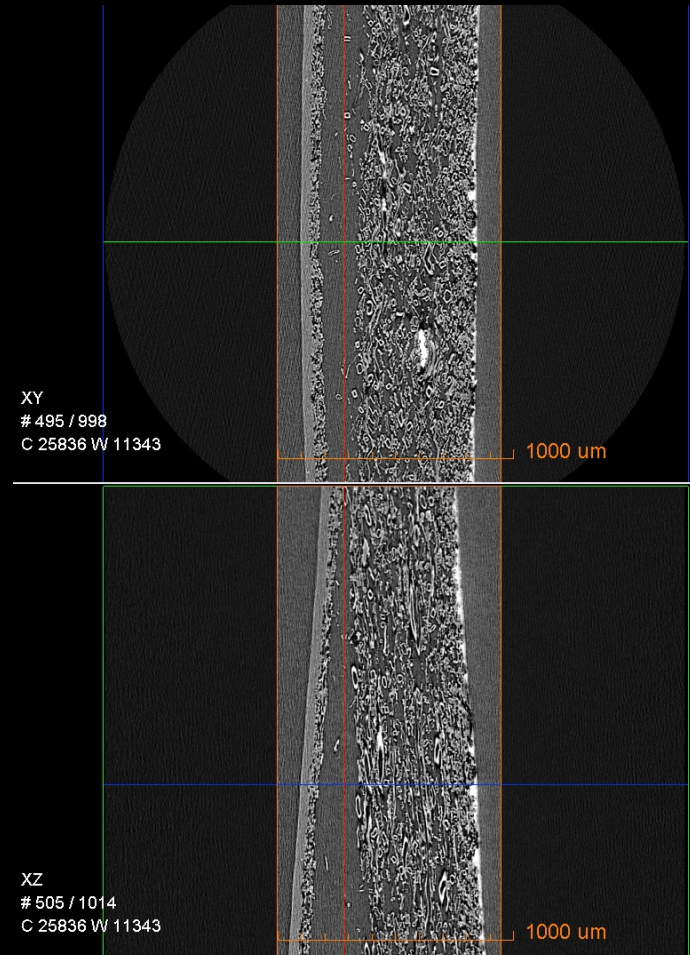


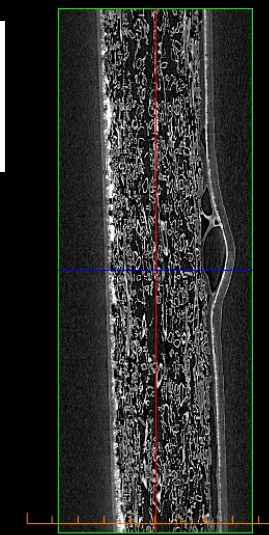
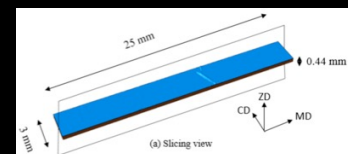
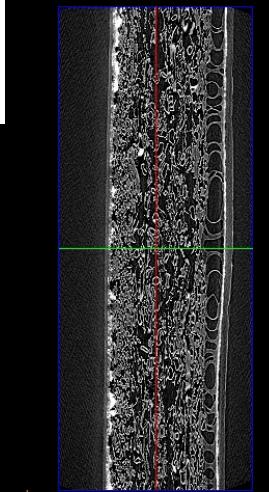
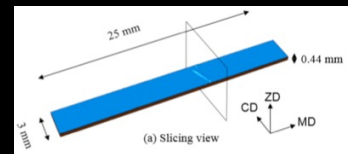
Image from Johansson & Dahlström,
MSc Thesis, Div. Solid Mechanics, LTH
In Collaboration with TetraPak

Blistering in Paperboard

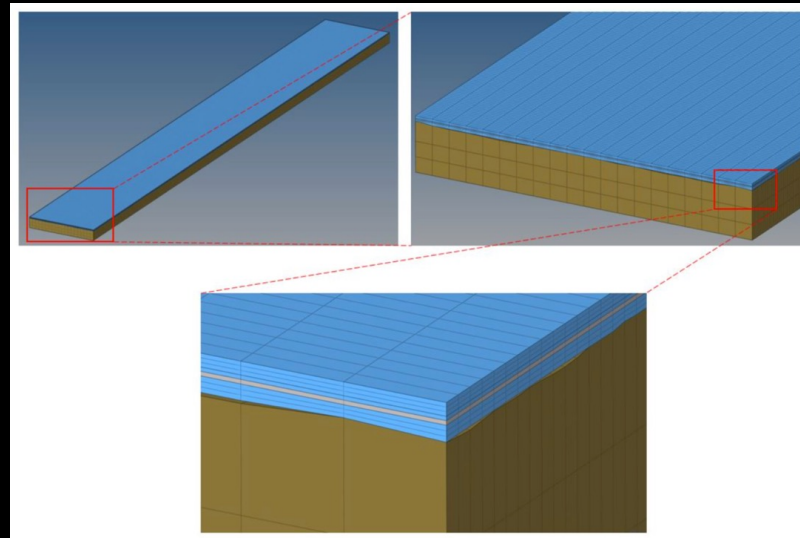
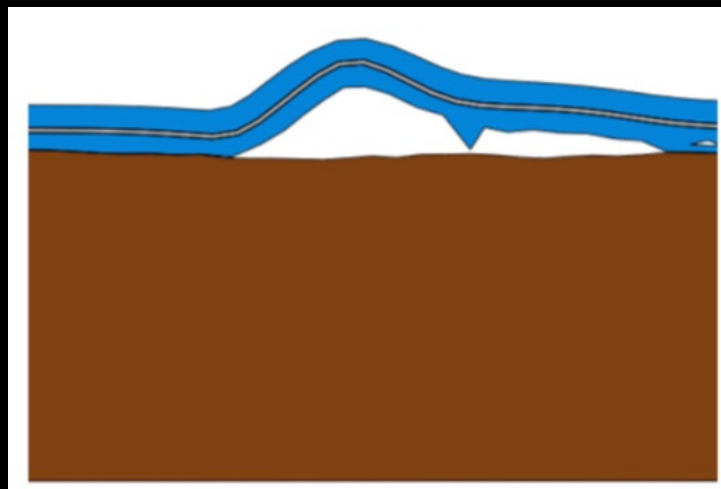
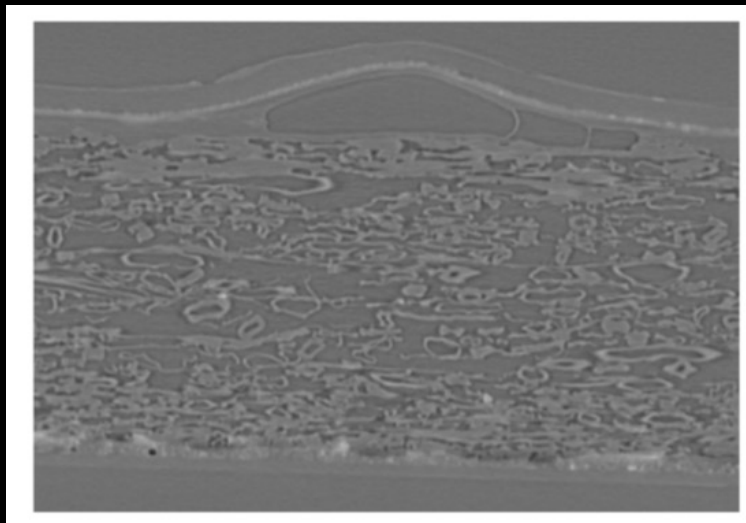


Collaboration with RISE / StoraEnso (SuMo Biomaterials)

Wrinkling in Paperboard



Wrinkling in Paperboard



Johansson & Dahlström, MSc Thesis,
Div. Solid Mechanics, LTH In
Collaboration with TetraPak





4D IMAGING LAB

A Lund university Infrastructure

vision of Solid Mechanics, LTH, Lund

www.solid.lth.se/resources/4d-imaging-lab/

Zeiss Xradia XRM 520



- High resolution 3D x-ray microscope
- 3D imaging resolutions down to < 700 nm (voxel sizes down to 70 nm)
- 30 – 160 kV
- Diffraction Contrast Tomography (DCT) capability

RXSolutions EasyTom150



- Large field of view (flat panel)
- 40- 150 kV
- Large working space
- Faster imaging



A
Treesearch
infrastruct
ure



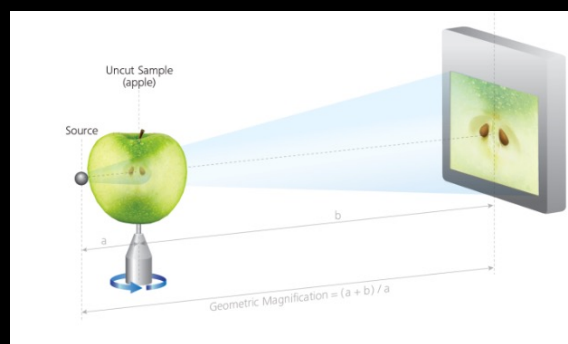
4D IMAGING LAB

A Lund university Infrastructure

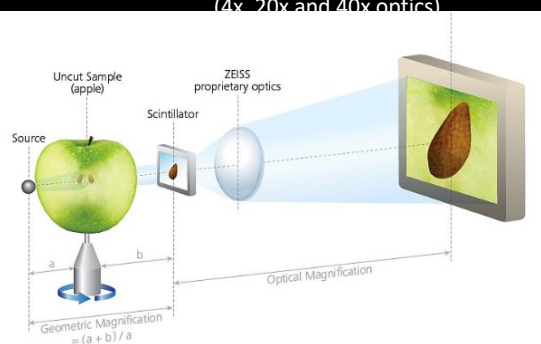
- Zeiss Xradia XRM 520 high resolution lab x-ray microscope



Geometrical magnification



Secondary optical magnification
(4x, 20x and 40x optics)



- High thermal and mechanical stability and high precision positioning
- High resolution CCD camera
- Small spot size (around 2 microns)
- 3D imaging resolutions down to < 700 nm

Images courtesy of Carl Zeiss Microscopy



4D IMAGING LAB

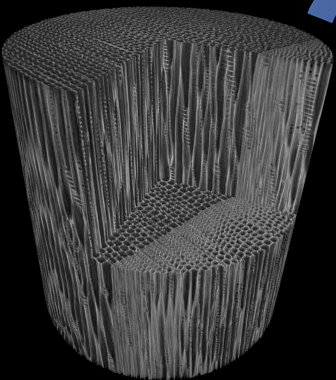
A Lund university Infrastructure

vision of Solid Mechanics, LTH, Lund

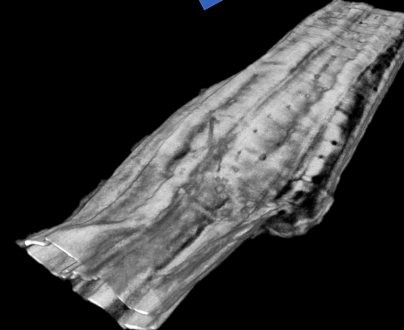
www.solid.lth.se/resources/4d-imaging-lab/



Tomographic image of
Spruce wood
FoV diameter = 49 mm



Tomographic image of a
sample of Spruce wood
FoV diameter = 1.5 mm



Tomographic image
of wood fibres
Voxel size = 300 nm
FoV = 300 microns

Multiscale

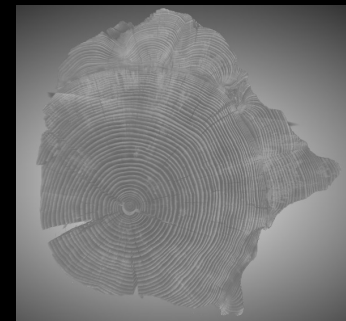


4D IMAGING LAB

A Lund university Infrastructure

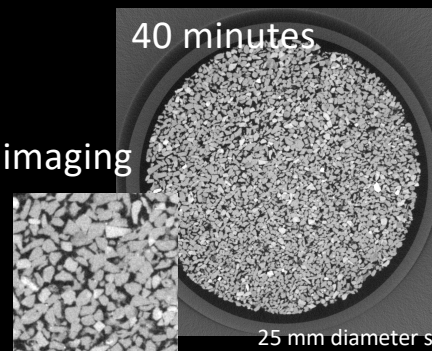
RXSolutions EasyTom150

Larger samples
300 mm x 450 mm

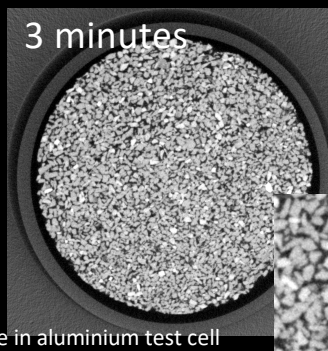


Faster imaging

40 minutes



3 minutes



25 mm diameter sandstone in aluminium test cell